NIH Public Access
Author Manuscript
J Am Chem Soc. Author manuscript; available in PMC 2010 April 8.

Published in final edited form as:
J Am Chem Soc. 2009 April 8; 131(13): 4729–4743. doi:10.1021/ja808698x.

Slow Hydrogen Transfer Reactions of Oxo— and Hydroxo—Vanadium Compounds: the Importance of Intrinsic Barriers

Christopher R. Waidmann[†], **Xin Zhou**[§], **Erin A. Tsai**[†], **Werner Kaminsky**[†,‡], **David A. Hrovat**[§], **Weston Thatcher Borden**[*,§], and **James M. Mayer**[*,†]

[†]Department of Chemistry, Campus Box 351700, University of Washington, Seattle, WA, 98195-1700

[§]Department of Chemistry, University of North Texas, P.O. Box 305070, Denton, TX 76203-5070

[‡]UW crystallographic facility

Abstract

Reactions are described that interconvert vanadium(IV) oxo-hydroxo complexes $[V^{IV}O(OH)(R_2bpy)_2]BF_4$ (**1a-c**) and vanadium(V) dioxo complexes $[V^{V}O_2(R_2bpy)_2]BF_4$ (**2a-c**) [R_2bpy = 4,4′-di-*t*-butyl-2,2′-bipyridine (^{t}Bu$_2$bpy), **a**; 4,4′-dimethyl-2,2′-bipyridine (Me$_2$bpy), **b**; 2,2′-bipyridine (bpy), **c**]. These are rare examples of pairs of isolated, sterically unencumbered, first-row metal-oxo/hydroxo complexes that differ by a hydrogen atom ($H^+ + e^-$). The V^{IV}– ^{t}Bu$_2$bpy derivative **1a** has a useful ^{1}H NMR spectrum, despite being paramagnetic. Complex **2a** abstracts H• from organic substrates with weak O–H and C–H bonds, converting 2,6-^{t}Bu$_2$-4-MeO-C$_6$H$_2$OH (ArOH) and 2,2,6,6-tetramethyl-*N*-hydroxy-piperidine (TEMPOH) to their corresponding radicals ArO• and TEMPO, hydroquinone to benzoquinone, and dihydroanthracene to anthracene. The equilibrium constant for **2a** + ArOH ⇋ **1a** + ArO• is $(4 \pm 2) \times 10^{-3}$, implying that the VO–H bond dissociation free energy (BDFE) is 70.6 ± 1.2 kcal mol^{-1}. Consistent with this value, **1a** is oxidized by 2,4,6-^{t}Bu$_3$C$_6$H$_2$O•. All of these reactions are surprisingly slow, typically occurring over hours at ambient temperatures. The net hydrogen-atom pseudo-self-exchange **1a** + **2b** ⇋ **2a** + **1b**, using the ^{t}Bu- and Me-bpy substituents as labels, also occurs slowly, with $k_{se} = 1.3 \times 10^{-2}$ M^{-1} s^{-1} at 298 K, $\Delta H^{\ddagger} = 15 \pm 2$ kcal mol^{-1}, and $\Delta S^{\ddagger} = 16 \pm 5$ cal mol^{-1} K. Using this k_{se} and the BDFE, the vanadium reactions are shown to follow the Marcus cross relation moderately well, with calculated rate constants within 10^2 of the observed values. The vanadium self-exchange reaction is ca. 10^6 slower than that for the related $Ru^{IV}O(py)(bpy)_2^{2+}$ / $Ru^{III}OH(py)(bpy)_2^{2+}$ self-exchange. The origin of this dramatic difference has been probed with DFT calculations on the self-exchange reactions of **1c** + **2c** and on mono-cationic ruthenium complexes with pyrrolate or fluoride in place of the py ligands. The calculations reproduce the difference in barrier heights and show that transfer of a hydrogen atom involves more structural reorganization for vanadium than the Ru analogs. The vanadium complexes have larger changes in the metal–oxo and metal–hydroxo bond lengths, which is traced to the difference in d-orbital occupancy in the two systems. This study thus highlights the importance of intrinsic barriers in the transfer of a hydrogen atom, in addition to the thermochemical (bond strength) factors that have been previously emphasized.

Introduction

The interconversion of metal-oxo and reduced metal-hydroxo complexes (eq 1) is of fundamental importance in chemistry, biology, and the environment. This is also perhaps the

*E-mail: borden@unt.edu, mayer@chem.washington.edu.

NIH-PA Author Manuscript
NIH-PA Author Manuscript
NIH-PA Author Manuscript

NIH-PA Author Manuscript

NIH-PA Author Manuscript

NIH-PA Author Manuscript

paradigmatic example of processes that involve transfer of both a proton and an electron.[1–5] In

$$M^{n+}=O + H\bullet \ (e^{-}+H^{+}) \rightleftarrows M^{(n-1)+} - OH \quad (1)$$

that context, reactions (1) have been called proton-coupled electron transfer (PCET), concerted proton electron transfer (CPET) and/or hydrogen atom transfer (HAT);[1–7] distinctions among these various terms are discussed below. Reaction (1) is particularly important in metal-mediated oxidation reactions, where metal-oxo complexes are able to abstract a hydrogen atom ($H\bullet \equiv e^{-} + H^{+}$) from a substrate, forming the corresponding hydroxo complex. This is thought to be the key step in hydrocarbon C–H bond oxidations by metalloenzymes such as cytochromes P450,[8] TauD,[9] soluble methane monooxygenase,[10] and class I ribonucleotide reductases.[11] This step is also involved in the oxidation of butane to maleic anhydride by an oxovanadium(V) catalyst (to cite one industrial example)[12] and in smaller-scale reactions of permanganate, oxochromium(VI) compounds, activated manganese dioxide, and other reagents.[13] Oxo-hydroxo interconversions also occur widely in the aqueous speciation of metals from vanadium to osmium.[14]

Given the importance of reactions that interconvert oxo and hydroxo species, there are few studies of systems where both the metal-oxo and metal-hydroxo compounds have been isolated and their hydrogen atom transfer reactivity studied. Meyer and others have developed an extensive reaction chemistry of polypyridyl ruthenium-oxo and -hydroxo complexes, where the ruthenium hydroxo species can be observed but are typically not isolable.[15] Bakac *et al.* have studied the hydrogen transfer reactions of transient chromium–oxo and –superoxo complexes.[16] Systems with isolable oxo and hydroxo species have been developed by Borovik (Fe, Mn) and by Theopold (Cr), using bulky supporting ligands and hydrogen bonding to prevent formation of dimers (which may also inhibit reactions with substrates).[17] In most other systems, the metal-oxo compounds are strong oxidants and/or the hydroxo compounds are unstable, for instance condensing to form μ-oxo species.

The recent synthesis of mononuclear vanadium(IV)-oxo-hydroxo-bipyridine compounds by Kabanos *et al.*,[18] coupled with the known vanadium(V)-dioxo-bipyridine compounds,[19] provide a rare example of an isolable 1st row metal-oxo/hydroxo system. Oxovanadium compounds, including polyoxometallates, have been extensively studied for a variety of reasons, including their insulin mimetic activity,[20] their presence in haloperoxidase enzymes,[21] and their utility for the catalytic oxidation of organic substrates.[12,22 − 26] Vanadium oxides are also valuable heterogeneous catalysts, as in butane oxidation mentioned above.[12],

Reported here are net hydrogen transfer reactions involving these relatively simple vanadium oxo and hydroxo complexes. This is part of recent emphasis, in our lab[27–32] and others,[1–3,15–17,33–37] on PCET/HAT/CPET reactions of metal coordination compounds, including iron, ruthenium, osmium, cobalt, nickel, manganese, copper, and chromium species. When the species that differ by a hydrogen atom (one e^{-} and one H^{+}) can be isolated and examined in detail, new understanding of such H· transfer reactions can be derived. We have emphasized the importance of thermochemistry in these reactions (the strength of the H–X bonds that are broken and formed) and we have found that the rate constants for many of these reactions roughly follow the Marcus cross relation.[2,29] Extending that work to this vanadium system, we have examined both cross reactions (eq 2, N–N = a bipyridine ligand) and self-exchange reactions, $L_n V{=}O + HO{-}VL_n \rightarrow L_n V{-}OH + O{=}VL_n$. The vanadium reactions are remarkably slow compared to other metal-mediated hydrogen transfer reactions. Most notably, the self-exchange occurs roughly a million times slower than the self-exchange between structurally related ruthenium oxo/hydroxo-bipyridine complexes. DFT calculations on models for the

NIH-PA Author Manuscript

NIH-PA Author Manuscript

NIH-PA Author Manuscript

vanadium and ruthenium self-exchange reactions reproduce this dramatic disparity and indicate that it results from differences in inner-sphere reorganization energies.

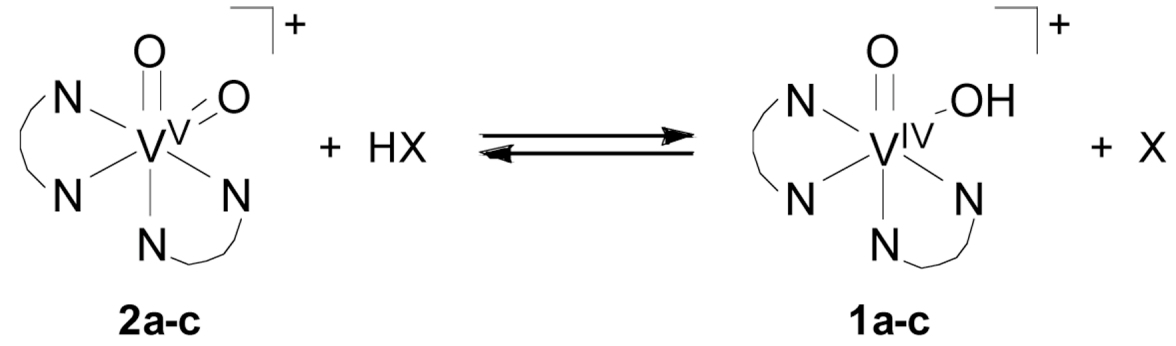

2a-c **1a-c**

(a) N—N = ^{t}Bu$_2$bpy, (b) N—N = Me$_2$bpy, (c) N—N = bpy

(2)

Results

1. Vanadium-oxo and -hydroxo complexes

have been prepared with 4,4′-di-*t*-butyl-2,2′-bipyridine (^{t}Bu$_2$bpy, **a** series), 4,4′-dimethyl-2,2′-bipyridine (Me$_2$bpy, **b**), and 2,2′-bipyridine (bpy, **c**). The vanadium(IV) oxo-hydroxo complexes [$V^{IV}O(OH)(R_2bpy)_2$]BF_4 (**1a–c**) reported by Kabanos *et al.*[18] have been made, using a revised procedure, from V(O)SO_4, HBF_4, $BaCO_3$, and the R_2bpy ligand. We also describe (see Experimental Section) an improved route[38] to the known[19] dioxovanadium(V) compounds [$V^{V}O_2(R_2bpy)_2$]BF_4 (**2a–c**), by adding two equivalents of ligand to aqueous HBF_4 solutions of $NaVO_3$ at pH = 1. The X-ray structure of **2c** (Figure 1; Table 1 below)[39] shows a cation with a distorted octahedral geometry. The two short V=O bonds of 1.627(5) Å are typical of $V^{V}O_2^{+}$ compounds and are similar to the two previously reported crystal structures of this cation (in compounds with different counterions prepared in less direct fashions).[19,40,41] The V–N bonds *trans* to an oxo are 0.15(3) Å longer than the V–N bonds trans to a bpy nitrogen, illustrating the strong *trans* influence of the oxo ligands.

Compounds **1** and **2** have been characterized by mass spectrometry, IR and ^{1}H NMR spectra, in addition to comparison of their optical spectra with those of reported derivatives. UV-Vis spectra of **2a–c** show strong peaks with $\lambda_{max} \leq$ ~350 nm (ε ~ 20 000 M^{-1} cm^{-1}) that tail into the visible. Compounds **1a–c** also show two d-d bands at *ca*. 520 and 750 nm (ε ~ 30 M^{-1} cm^{-1}), as expected for octahedral oxovanadium(IV) complexes.[42] All the IR spectra show strong vanadium-oxo stretching modes, with the one stretch for the vanadyl compounds **1a–c** ($\nu_{V\equiv O}$ *ca*. 970 cm^{-1}) at higher energy than the symmetric and antisymmetric stretches for **2a–c**(ν_{VO_2} *ca.* 930, 910 $cm^{02212;1}$).[40] Cyclic voltammograms of **1a** in MeCN show a wave that is chemically reversible at high scan rates, with $E_{1/2}$ = 1.065 V vs. $Cp_2Fe^{+/0}$(Figure S1 and Figure S2), and a number of features below −1 V.[39] CVs of **2a** show no reduction wave between 2 and −1 V vs. $Cp_2Fe^{+/0}$. Below −1 V, CVs of **2a** have reduction waves identical to those of **1a** even with efforts to remove all proton sources. Complex **2a** reacts only very slowly with Cp_2Fe in MeCN, indicating that its $E_{1/2}$ is < 0 V vs. $Cp_2Fe^{+/0}$. The aqueous electrochemistry of the bipy complexes **1c** and **2c**, the only derivatives with appreciable solubility in water,

NIH-PA Author Manuscript

NIH-PA Author Manuscript

NIH-PA Author Manuscript

showed an irreversible, pH-independent oxidation at 0.68 V vs. $Cp_2Fe^{+/0}$ (as well features below −1 V similar to those observed in MeCN).

The ^{1}H NMR spectra of the dioxo complexes **2a–c** at 295 K all have three or four very broad resonances in the aryl region, indicating that all the R-py rings are equivalent on the NMR timescale. Upon cooling, the peaks sharpen and separate into two sets of pyridine resonances, as shown in Figure 2 for **2a**. Assignments were made using 2D COSY and NOESY experiments at 190 K in CD_2Cl_2. Raising the temperature of CD_3CN solutions to 340 K causes the ^{t}Bu resonances of **2a** to coalesce and then sharpen, although the aryl peaks remain broad. The spectra indicate that the $[VO_2(R_2bpy)_2]^+$ cations have the expected C_2 structure in solution (as found in the solid state, Figure 1) and have a fluxional process which equilibrates the pairs of R-py rings. Line shape analysis of spectra of **2a** in CD_2Cl_2 from 190 to 300 K gives the Eyring parameters $\Delta H^{\ddagger} = 18 \pm 2$ kcal mol^{-1} and $\Delta S^{\ddagger} = 14 \pm 2$ cal mol^{-1} K^{-1} for the fluxional process. Complex **2b** behaves similarly ($\Delta H^{\ddagger} = 16 \pm 2$ kcal mol^{-1}, $\Delta S^{\ddagger} = 9 \pm 2$ cal mol^{-1} K^{-1}), while **2c** is insoluble in CD_2Cl_2. The spectra are similar in CD_3CN for all three compounds, with broad peaks of similar linewidths at ambient temperature that sharpen but do not reach the low temperature limit at 235 K. The positive entropies and large *trans* influence, as evidenced by the structure of **2c**, suggest a dissociative mechanism.

$[V^{IV}O(OH)(^tBu_2bpy)_2]BF_4$ (**1a**) has a useful and characteristic ^{1}H NMR spectrum despite being a d^1 paramagnet. Four peaks are observed between 1 and 4 ppm (Figure 3), assigned to the four inequivalent ^{t}Bu groups. No other resonances are discernable between +100 and −100 ppm. The observation of 4 ^{t}Bu resonances indicates that exchange of the proton between the hydroxo and oxo moieties is slow on the NMR timescale. While proton transfer between oxygens is usually very rapid, slow exchange has previously been described for other oxo-hydroxo compounds.[43] The one broad ^{t}Bu resonance, labeled 4 in Figure 3, is tentatively assigned to the ^{t}Bu on the pyridine ring that is coplanar with the vanadyl group, because only this pyridine has overlap of its π system with the vanadium d_{xy} orbital that holds the unpaired electron.[18] The ^{1}H NMR spectrum of **1b** shows only two very broad peaks between 2 and 5 ppm (likely due to the Me groups) and compound **1c** does not show a ^{1}H NMR spectrum.

Solutions of the dioxo compounds **2a–c** in organic solvents decompose over the course of days at ambient temperatures. The decomposition appears to be faster at higher concentrations and elevated temperatures, and is evidenced by a change in the color of solution from pale yellow to green. Decomposition appears to give primarily $[V^{IV}O(OH)(R_2bpy)]^+$ (**1a–c**), by NMR. While the other products have not been identified, oxo-bridged vanadium dimers are often green.[44,45] Compounds **1a–c** are stable in solution for a week at room temperature.

2. Hydrogen atom self-exchange

^{1}H NMR spectra of CD_3CN and CD_2Cl_2 solutions containing both **1a** and **2a** are essentially the sum of the spectra of the two species. There is no evidence for any chemical exchange process, even at 340 K when the spectrum of **1a** is fairly sharp (Figure 2). This indicates that degenerate hydrogen atom self-exchange between the *cis*-oxo-hydroxo-vanadium(IV) and *cis*-dioxovanadium(V) compounds **1a** and **2a** is slow on the NMR timescale, too slow to measure by NMR line broadening. This result is surprising because we have used NMR line broadening to measure self-exchange rate constants in a number of related systems.[46]

We have therefore examined the reaction between **1a** and **2b** to give **1b** and **2a**, and the reverse (Scheme 1). This can be considered a pseudo self-exchange reaction because the alkyl substituents are electronically similar (Me vs. ^{t}Bu) and are distant from the reacting centers. The reaction was monitored by ^{1}H NMR because three of the four species have characteristic resonances (**1a**, **2a** and **2b**). Because of the broad spectra of **2a** and **2b** near 300 K (Figure 2), these experiments must be done either at elevated or lower temperatures, to sharpen the ^{t}Bu

NIH-PA Author Manuscript

NIH-PA Author Manuscript

NIH-PA Author Manuscript

peaks of **2a**, which would otherwise obscure the ^{t}Bu peaks of **1a**. Figure 4 shows a portion of the NMR spectra for a reaction at 320 K, in which the three narrower ^{t}Bu resonances of **1a** convert to the single ^{t}Bu peak of **2a** at δ1.45. Over the course of these reactions, a small amount of free ^{t}Bu$_2$bpy ligand (1–5%) is observed as a sharp peak at δ1.40, its diamagnetic signal higher than the broader peaks despite its low concentration. The integrals of the NMR resonances were determined using the line-fitting tool of MestreC.[47] Plots of concentrations *vs*. time, such as Figure 5a, illustrate the good mass balance in these reactions: in all of the reactions, the sum of the concentration of ^{t}Bu$_2$bpy species ([**1a**] + [**2a**]) remains constant within error.

The kinetic data fit well to a second-order approach to equilibrium model, which yields both equilibrium and rate constants K_{se} and k_{se}.[48] The same K_{se} and k_{se} were found from reactions done in either direction and with various starting conditions, including beginning with three species present initially. Over the entire 280–320 K temperature range, the equilibrium constants are 1.0 ± 0.6 indicating that these are very close to true self-exchange reactions. k_{se} at 320 K in anhydrous CD_3CN is $(1.0 \pm 0.3) \times 10^{-1}$ M^{-1} s^{-1}. Eyring analysis of rate constants at 280 and 310–330 K gives $\Delta H^{\ddagger} = 15 \pm 2$ kcal mol^{-1} and $\Delta S^{\ddagger} = -16 \pm 5$ cal mol^{-1} K^{-1}.[49] These values give a rate constant at 298 K (which is not directly measurable, see above) of $k_{se} = (1.3 \pm 0.1) \times 10^{-2}$ M^{-1} s^{-1}. This is a remarkably slow reaction, more than a million times slower than the sterically similar self-exchange reaction of $Ru^{IV}O(py)(bpy)_2^{2+}$ + $Ru^{III}(OH)(py)(bpy)_2^{2+}$;[28] this comparison will be developed below. At 320 K, the reaction proceeds very similarly in CD_2Cl_2 giving $k_{se}(CD_2Cl_2) = (1.7 \pm 0.2) \times 10^{-1}$ M^{-1} s^{-1}, 1.7 times faster than in CD_3CN. Addition of H_2O up to a concentration of 0.5 M (100 equivalents) slowed the rate in CD_3CN by a factor of 1.6. The same rate within error was observed when D_2O was added, indicating a kinetic isotope effect of close to unity. There is no indication, from either the NMR or the kinetic data, for initial formation of a hydrogen-bonded adduct between the hydroxo complexes **1** and the oxo complexes **2**. A stable complex involving paramagnetic **1** would likely broaden the resonances for **2**, but no broadening is observed in mixtures of **1** and **2**. The negative activation entropy of $\Delta S^{\ddagger} = -16 \pm 5$ cal mol^{-1} K^{-1} also suggests that the reaction proceeds from separated **2b** + **1a**.

3. Hydrogen atom transfer cross reactions

Reactions of **1a** and **2a** with hydrogen atom donors and acceptors have been explored, taking advantage of their good solubility and distinctive optical and ^{1}H NMR spectra. Complex **2a** oxidizes hydroquinone in CD_3CN to give benzoquinone and **1a**, in ~80% yield by ^{1}H NMR (eq 3; N–N = ^{t}Bu$_2$bpy). With stoichiometric amounts of reactants at 10 mM concentrations, the reaction requires several hours to reach completion at ambient temperatures. UV-vis spectra of reaction 3 show formation of **1a**, benzoquinone, and an unidentified species with a strong absorbance extending from 380 nm into the visible region.[39] This unknown species is not formed from **2a** plus the product benzoquinone, nor from **1a** plus hydroquinone, as neither of these reactions show any discernable change over 24 h by ^{1}H NMR and UV-Vis. Monitoring the kinetics by ^{1}H NMR, the rate of disappearance of hydroquinone under pseudo-first order conditions of excess **2a** suggests a rate constant of $(4.0 \pm 0.5) \times 10^{-2}$ M^{-1} s^{-1} for reaction 3, assuming a bimolecular rate-limiting step.[39]

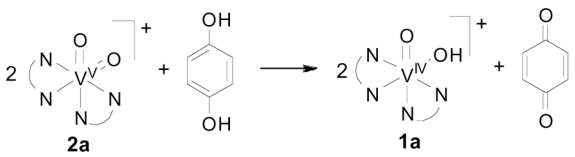

(3)

NIH-PA Author Manuscript

NIH-PA Author Manuscript

NIH-PA Author Manuscript

Complex **2a** also slowly oxidizes 2,6-di-*tert*-butyl-4-methoxyphenol (ArOH), with **1a** appearing over a period of hours at NMR concentrations in CD_3CN at 298 K (eq 4). Optical spectra of the reaction show the distinct spectrum of the phenoxyl radical, which is quite stable (Figure 6).[50] The formation of **1a** and ArO• indicates that net H-atom transfer has occurred. Much less than a stoichiometric amount of radical is formed, however. At [**2a**] = 1.1 mM, 3.0 mM ArOH gives a 3.6% yield of ArO• (in 4000 seconds), while 45 mM ArOH gives 25% ArO•. Less phenoxyl is formed when **1a** is present initially: 1.9 mM **2a** plus 5.4 mM ArOH gives 3% ArO•, but only 0.6% ArO• when 1.9 mM **1a** is added. These and fifteen other measurements, spanning an order of magnitude in [**2a**] and [ArOH], indicate that equilibrium is reached with $K_4 = (4 \pm 2) \times 10^{-3}$ in CH_3CN at 298 K, $\Delta G_4 = 3.3 \pm 0.5$ kcal mol^{-1}. ArOH has a weak O–H bond, with a bond dissociation free energy in MeCN (BDFE) of 73.9 ± 1 kcal mol^{-1},[51] from this the VO-H BDFE of **1a** can be calculated as 70.6 ± 1.2 kcal mol^{-1}. The kinetics, monitored by UV-vis spectroscopy and analyzed using SPECFIT,[52] fit well to a second-order approach to equilibrium model with $k_4 = (1.4 \pm 0.5) \times 10^{-3}$ M^{-1} s^{-1}.

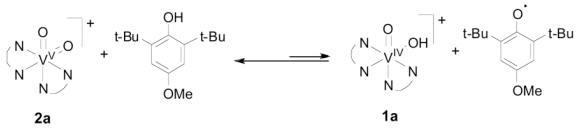

(4)

In contrast, **2a** does not react with 2,4,6-tri-*tert*-butylphenol (^{t}Bu$_3$ArOH) in MeCN. Neither the UV-vis spectrum of **1a** nor the distinct sharp UV spectrum of the stable radical ^{t}Bu$_3$PhO• are observed in millimolar solutions of these reagents. The reverse reaction, ^{t}Bu$_3$PhO• plus **1a**, does proceed slowly. For instance, a solution of 3 mM **1a** and 30 mM ^{t}Bu$_3$PhO• in CD_3CN showed a 20% yield of **2a** by NMR after several days, although many side products were also observed. This is the only case where H-atom abstraction from **1a** has been observed (reactions of ^{t}Bu$_2$(MeO)C$_6$H$_2$O• are problematic because the radical solutions contain excess phenol). The different position of the equilibria for **2a** + ^{t}Bu$_3$ArOH *vs*. **2a** + ^{t}Bu$_2$(MeO)C$_6$H$_2$O• is consistent with the 3 kcal mol^{-1} higher O–H BDFE of ^{t}Bu$_3$ArOH in MeCN, 77 ± 1 kcal mol^{-1}.[53,54]

The hydroxylamine TEMPOH (2,2,6,6-tetramethyl-*N*-hydroxy-piperidine), which has an O-H BDFE of 66.5 ± 0.5 kcal mol^{-1},[29,55] also slowly reduces **2a** to **1a**. This reaction is however complicated by the further reaction of **1a** with TEMPOH. ^{1}H NMR spectra of 7 mM **2a** plus 73 mM TEMPOH at 275 K showed complete disappearance of **2a** within 3 h but the maximum yield of **1a** was only 30% and other products are observed, including free ^{t}Bu$_2$bpy.[39] With a larger excess of TEMPOH, **2a** is consumed faster but the yield of **1a** is no higher. These issues have prevented quantitative studies but the data are qualitatively consistent with a bimolecular rate constant of ca. 10^{-1} M^{-1} s^{-1}. TEMPOH and hydroquinone seem capable of coordinating and displacing ^{t}Bu$_2$bpy, while this seems to be prevented by the 2,6-di-*t*-butyl groups of the phenols.

Complex **2a** is also slowly reduced by xanthene and dihydroanthracene (DHA). A sealed NMR tube containing 13 mM **2a** and 51 mM DHA showed stoichiometric 20% conversion to anthracene and a corresponding amount of **1a** after 2.5 days at 298 K by ^{1}H NMR, but further reaction is complicated by the decomposition of **2a**. Xanthene reduces **2a** more quickly, with 45% conversion to **1a** in 30 hours under similar conditions. Within 7 days, **2a** is quantitatively reduced to **1a**, and 5% free ligand is observed. No xanthone or anthrone are observed in these reactions.[56] The kinetics of **2a** + xanthene were followed by the stoichiometric growth of the d-d band of **1a** at 754 nm (Figure S10[39]). The pseudo-first order k_{obs} varied linearly with

NIH-PA Author Manuscript

NIH-PA Author Manuscript

NIH-PA Author Manuscript

[xanthene], yielding $k_{xan} = (7.6 \pm 2.4) \times 10^{-5}$ M^{-1} s^{-1}. The more limited data for the DHA reaction are consistent with $k_{DHA} \sim 2 \times 10^{-6}$ M^{-1} s^{-1}. The xanthene C-H BDFE is 70.9 kcal mol[1,28,57] so H• transfer from xanthene to **2a** is essentially thermoneutral; the reaction is presumably driven by further reactions of the xanthyl radical.

4. DFT Calculations

Hydrogen atom self-exchange between **1c** and **2c** has been examined using DFT calculations, which were performed with the B3LYP functional[58] and the 6-31G* basis set.[59] The polarizable continuum model (PCM)[60] was used to approximate the effects of solvation in acetonitrile. All of the calculations were carried out with the Gaussian03 package of programs.[61]

Gas phase structures of the **1c** and **2c** cations were calculated, and their bond lengths and angles are listed with the experimental solid-state structures of the BF_4 salts in Table 1. For **1c**, the calculated V=O is close to that expected for a V^{IV}=O distance.[62] The experimental V=O and V–OH distances are unusually long and short, respectively (as was noted in reference [18a]), perhaps reflecting some disorder in the crystal.

Bringing complexes **1c** and **2c** together forms a hydrogen-bonded 'precursor complex,' in which the hydroxo group of **1c** acts as a hydrogen bond donor to one of the oxo groups of **2c**. Formation of this precursor complex is calculated to be endothermic by 17.9 kcal mol^{-1} in the gas phase, due to the large Coulombic repulsion between the positively charged vanadium reactants. Solvation reduces this Coulombic repulsion, as formation of the hydrogen-bonded precursor complex is calculated to be exothermic by −4.7 kcal mol^{-1} in acetonitrile. This negative $\Delta H°$ in acetonitrile is counteracted by the positive entropy of formation, which is calculated (in the gas-phase) as $\Delta S° = -36.8$ cal mol^{-1} K^{-1}, so $\Delta G°$ is calculated to be positive, 6.8 kcal mol^{-1}. Thus, the calculations find that the ground state of the system is the separated reactants, not the hydrogen-bonded complex, consistent with experimental observations.

Transition state structures for hydrogen exchange between **1c** and **2c** were also calculated. In acetonitrile, $\Delta H^{‡}$ for formation of the C_2 symmetric transition structure, in which the proton is halfway between the oxygen atoms, is calculated to be 12.4 kcal mol^{-1} above the separated reactants and 17.1 kcal mol^{-1} above the hydrogen-bonded complex. This value of $\Delta H^{‡}$ = 12.4 kcal mol^{-1} for reaction of **1c** and **2c** is in reasonable agreement with the experimental value of $\Delta H^{‡} = 15 \pm 2$ kcal mol^{-1} in MeCN.

Interestingly, the calculated gas-phase value of $\Delta H^{‡}$ = 16.3 for degenerate hydrogen atom exchange from the hydrogen-bonded precursor complex is nearly the same as the PCM value. Thus, although the PCM and gas-phase values for formation of the hydrogen-bonded complex differ by 22.6 kcal mol^{-1}, the PCM and gas-phase values of for $\Delta H^{‡}$ for hydrogen exchange differ by only 0.8 kcal mol^{-1}. The presence of a polar solvent is calculated to stabilize the precursor complex and transition structure almost equally, so the solvent has very little effect on the barrier for hydrogen exchange within the complex.

The calculated C_2 transition structure[63] has a nearly linear O–H–O bridge (see Table 1 and Figure 11 below). The two vanadium centers are twisted about this bridge, with a calculated O=V---V=O torsion angle of 124.2°. The V–O bonds involved in the H transfer are calculated to be 1.710 Å long at this transition state, intermediate between the calculated lengths of 1.859 and 1.595 Å for the V–OH and V=O bond lengths of isolated **1c** and **2c**, respectively.

As mentioned in the previous section, the reaction of **1a** with **2b** is much slower than the apparently similar self-exchange reaction of $Ru^{IV}O(py)(bpy)_2^{2+}$ with $Ru^{III}(OH)(py)(bpy)_2^{2+}$.[28] Unfortunately, computational comparison of the reaction between **1c** and **2c** and

NIH-PA Author Manuscript

NIH-PA Author Manuscript

NIH-PA Author Manuscript

this ruthenium self-exchange reaction proved problematic, due to the dicationic nature of the ruthenium complexes. The dipositive charges on each of the separated Ru^{+2} reactants resulted in very strong electrostatic repulsion between them, so that neither a hydrogen-bonded complex nor a true transition state for the ruthenium self-exchange reaction could be located. Therefore, model systems were chosen,[64] in which the neutral pyridine ligand was replaced with a fluoride or pyrrolate ligand.[65] The resulting ruthenium reactants are, like their vanadium counterparts, monocationic; so hydrogen-bonded complexes and transition structures for hydrogen exchange could be located for both the ruthenium fluoride and ruthenium pyrrolate complexes.

Formation of these hydrogen-bonded precursor complexes in the gas phase is calculated to be endothermic by 15.5 kcal mol^{-1} for $Ru^{IV}(O)F(bpy)_2^+ + Ru^{III}(OH)F(bpy)_2^+$ [henceforth abbreviated as Ru(O)F + Ru(OH)F], and by 12.6 kcal mol^{-1} for $Ru^{IV}O(pyrr)(bpy)_2^+$ plus $Ru^{III}(OH)(pyrr)(bpy)_2^+$ [henceforth abbreviated as RuO(pyrr) + Ru(OH)(pyrr), pyrr = pyrrolate]. However, PCM calculations predict that in acetonitrile solution, formation of these hydrogen-bonded complexes should be exothermic with $\Delta H°$ = −5.2 and −8.7 kcal mol^{-1}, respectively. Thus, the effect of acetonitrile solvation on the enthalpies of formation of the ruthenium precursor complexes is calculated to be $\Delta H°$ = −20.7 and −21.3 kcal mol^{-1}. Both of these values are very similar to $\Delta H°$ = −22.6 kcal mol^{-1}, computed for solvation of the vanadium precursor complex.

C_2 symmetric transition state structures were also located for both ruthenium model complexes. The transition structures are calculated to be higher in enthalpy than the precursor complexes by 10.3 kcal mol^{-1} (F) and 12.1 kcal mol^{-1} (pyrr) in the gas-phase and by 11.1 and 12.6 kcal mol^{-1} in acetonitrile solution. Thus, as in the reaction of vanadium complexes **1c** and **2c**, solvation by acetonitrile is calculated to have a large enthalpic effect on formation of the ruthenium complexes, but only a very small effect on the barrier to degenerate hydrogen exchange reactions in the ruthenium complexes.

Figure 7 gives the differences between the calculated activation enthalpies for degenerate exchange in the hydrogen-bonded vanadium and ruthenium complexes in both acetonitrile solution and in the gas-phase. Starting either with the isolated reactants or with the hydrogen-bonded complexes, the activation enthalpy is much larger for hydrogen exchange between vanadium complexes **1c** and **2c** than between RuO(F) and Ru(OH)(F) or RuO(pyrr) and Ru(OH)(pyrr). For example, the enthalpic barrier to hydrogen exchange is 6.0 kcal mol^{-1} higher for **1c** + **2c** than for RuO(F) + Ru(OH)(F), even though in MeCN the enthalpies of formation of the hydrogen-bonded precursor complexes are only 0.5 kcal mol^{-1} smaller for **1c** + **2c** than for RuO(F) + Ru(OH)(F). The same 6.0 kcal mol^{-1} difference in barrier heights is also computed for the gas-phase reactions, indicating that the difference is not due to solvation. Nor is the difference in barrier heights due to zero-point energies or to heat capacities, because, if electronic energies are substituted for enthalpies, the 6.0 difference in activation enthalpies is reduced, but by only 0.2 kcal mol^{-1}.

Discussion

I. Cross reactions involving transfer of a hydrogen atom

Compound **2a** abstracts a hydrogen atom from the weak O–H or C–H bonds in a number of organic substrates. Complex **1a** and the oxidized organic substrate are formed (Scheme 2, Table 2), although the yields are sometimes low due to the sluggish nature of the reactions and competing decomposition. The reactive substrates have low O-H or C-H bond dissociation free energies (BDFEs[66]), ranging from 66.5 to 78 kcal mol^{-1}.[28,29,51,53–57,67,68] The O–H BDFE in **1a** was determined to be 70.6 ± 1.2 kcal mol^{-1} from the equilibrium **2a** + $^tBu_2$(MeO)ArOH ⇌ **1a** + $^tBu_2$(MeO)ArO•.[51]

NIH-PA Author Manuscript

NIH-PA Author Manuscript

NIH-PA Author Manuscript

These vanadium reactions are remarkably slow. Similar hydrogen transfer reactions (eq 5) have been examined for a wide variety of metal coordination complexes, including Cr, Mn, Fe, Ni, Co, Cu, Ru and Os complexes.[1–3,15,16,27–37] These reactions all involve redox change at the metal center, coupled with protonation or deprotonation of a ligand (eq 6).[69] A variety of ligands

$$X+HY \rightarrow XH + Y \quad (5)$$

$$L_xM^{n+}(X) + HY \rightarrow L_xM^{(n-1)+}(XH) + Y \quad (6)$$

act as the proton acceptor: oxo (bridging or terminal), alkoxy, superoxo, anilide, hexafluoro-acetylacetonate, imidazolate, imidazolinate, and terpyridine-4-carboxylate. Hydrogen transfer reactions of these complexes are typically rapid at modest driving forces when H• moves between electronegative oxygen or nitrogen atoms, reaching completion in seconds or less at room temperature and common concentrations ($k = 10^1$ to 10^6 M^{-1} s^{-1}). (Two exceptions are described below.) However, to our surprise, the reactions of the vanadium complexes **1a** and **2a** with oxyl radicals or O–H bonds are much slower, occurring over periods of hours to days at typical reactant concentrations, with rate constants of 10^{-4} to 10^{-1} M^{-1} s^{-1}.

The mechanisms of the reactions of **1** and **2** could involve concerted (one kinetic step) or stepwise transfer of the two particles (*cf.* [1,4–56,70,71]). Here, the stepwise paths would require high-energy intermediates. Stable vanadium-oxo compounds are predominantly either vanadium(IV) mono-oxo (vanadyl) or vanadium(V) polyoxo (many are *cis*-dioxo) complexes.[72] Initial electron transfer to **2a** would make $[V^{IV}(O)_2(N\text{-}N)_2]$, which is not easily generated from **2a**, as described above. Initial proton transfer to **2a** would give $[V^{V}(O)(OH)(N\text{-}N)_2{}^{2+}]$, a high energy species based on its estimated p$K_a$$[V^{V}O(OH)(^{t}Bu_2bpy)^{2+}]$ of −7 ± 2 (derived from a thermochemical cycle using the O-H BDFE and $E_{1/2}$ of **1a**, Scheme S1).[39] In addition, none of the substrates in Scheme 2 are good outer-sphere reductants ($E_{1/2}$ values from 0.7 to ~1.5 V versus $Cp_2Fe^{+/0}$[5,51c,73,74,75]) or strong acids (pK_a values from 28 to 40[51b,54,76,77]). The data thus indicate that initial proton or electron transfer from any of these substrates to **2a** would be very unfavorable, and that the reactions must therefore proceed by concerted transfer of e^- and H^+.

II. Pseudo Self-Exchange Reaction

Self-exchange rate constants provide a measure of the intrinsic ability of a reagent to undergo a particular reaction, in this case hydrogen transfer. In the vanadium-oxo system, self-exchange of a hydrogen atom is remarkably slow, based on the pseudo self-exchange reaction between the $^{t}Bu_2bpy$ and Me_2bpy derivatives, **1a** + **2b** → **1b** + **2a** (Scheme 1). This reaction, with k = (1.3 ± 0.1) × 10^{-2} M^{-1} s^{-1} and K_{eq} = 1.0 ± 0.6 in MeCN at 298 K, is much slower than related self-exchange reactions involving NH and OH moieties, as shown in Table 3. The closest analogy is the hydrogen atom self-exchange between $Ru^{IV}(O)(py)(bpy)_2{}^{2+}$ and $Ru^{III}(OH)(py)(bpy)_2{}^{2+}$, which occurs at (7.6 ± 0.4) × 10^4 M^{-1} s^{-1}.[28a] This value is *6 × 10^6times* faster than the vanadium self-exchange measured here. The Ru and V systems are both oxo/hydroxo interconversions and both have bis(bipyridine) supporting ligands; they differ only in the sixth ligand (oxo for V, pyridine for Ru) and the d-electron count ($d^{0/1}$ vs. $d^{4/5}$). The origin of this difference, and the slowness of the V systems, is discussed below.

The $V^{IV}O(OH)/V^{V}O_2$ self-exchange is slower than all but one of the hydrogen atom self-exchange reactions shown in Table 3 by a factor of *ca.* 10^5 or more. This large difference is seen in comparisons of reactions involving first-row and second-row metals, with terminal and

NIH-PA Author Manuscript

NIH-PA Author Manuscript

NIH-PA Author Manuscript

bridging oxo complexes, in a variety of steric environments, with neutral and multiply charged complexes, and in purely organic reactions. For example, self exchanges between protonated ketyl radicals and ketones, which are similar to $V^{IV}O(OH)/V^{V}O_2$ as Ė–OH + E=O processes, occur with rate constants of $(3.7 – 8.6) \times 10^3$ M^{-1} s^{-1}.[78] The self-exchange rate constants for other oxo/hydroxo couples, crudely estimated using the Marcus cross relation and measured cross-reaction rate constants, all occur rapidly, with $k \gtrsim 10^3$ M^{-1} s^{-1}. Self-exchange rate constants for reactions involving N–H bonds of metal-containing compounds range from 3.2×10^5 to 9.7×10^2 M^{-1} s^{-1},[30,31,70] with two exceptions. Self-exchange involving Co^{II}– and Co^{III}–tris(biimidazoline) complexes is slow, apparently due to the spin-change between low-spin Co^{III} and high-spin Co^{II} and the attendant large reorganization energy.[30a] H-transfer between Os(IV)-anilide and Os(III)-aniline complexes is also very slow ($k_{se} \leq 1.5 \times 10^{-3}$ M^{-1} s^{-1}), apparently due to strong steric crowding about the aniline hydrogen atoms.[31]

The very slow $V^{IV}O(OH)/V^{V}O_2$ self-exchange rate could have a number of origins. Hydrogen bond accepting solvents have been shown to significantly slow rates of hydrogen atom transfer, particularly for phenols, by forming an unreactive hydrogen-bonded complex XH ···solvent.[71] However, this is not significant for $V^{IV}O(OH)/V^{V}O_2$, as the self exchange is only 1.7 times faster in methylene chloride than in acetonitrile. This small solvent effect also supports a symmetrical transition structure, with little change in charge, rather than a stepwise mechanism of initial e^- or H^+ transfer.[71]

Steric crowding can slow rates of hydrogen transfer,[31,69c] but that seems unlikely here because the O-H and O moieties of $V^{IV}O(OH)$ and $V^{V}O_2$ are uncrowded (see Figure 1). In addition, $Ru(OH)(bpy)_2(py)^{2+}$ + $Ru(O)(bpy)_2(py)^{2+}$ self-exchange is much more facile, despite having *more* steric congestion around the oxygen atoms.

Small rate constants could also be a result of the vanadium reaction being nonadiabatic, such that the probability of crossing from reactant to product surfaces is small ($\kappa \ll 1$ in transition state theory).[79] This should result in a small Arrhenius prefactor A, which is equivalent to an unusually large negative activation entropy $\Delta S^{\ddagger}$. However, the values found for **1a** + **2a** self exchange, $A = 4 \times 10^9$ s^{-1}, $\Delta S^{\ddagger} = -16 \pm 5$ cal mol^{-1} K^{-1}, are typical of an adiabatic bimolecular reaction.[80] Therefore, large non-adiabatic contributions to the slow self-exchange are unlikely.

The slow vanadium self-exchange rate appears to be due almost entirely to a large activation barrier, $\Delta H^{\ddagger} = 15 \pm 2$ kcal mol^{-1} (Arrhenius $E_a = 15.4 \pm 2$ kcal mol^{-1}). In terms of Marcus theory, the high barrier indicates an adiabatic self-exchange reaction with a large intrinsic barrier, λ. As discussed below, this interpretation is supported by both the experimental results described in the next section, and by the DFT calculations that follow it.

III. Application of the Marcus Cross Relation

We have shown that the Marcus cross relation (eq 7) holds for many although not all hydrogen transfer reactions, [28–31,46b] even though it is a simplistic treatment.[81]Equation 7 predicts the rate constants for XH + Y → X + HY cross reactions (k_{xy}) in terms of its driving force (K_{eq}) and the self-exchange rate constants (k_{xx}, k_{yy}).[82,83]

$$k_{xy} = \sqrt{k_{xx} k_{yy} K_{eq} f_{xy}} \tag{7}$$

Cross rate constants have been calculated for the five vanadium reactions reported here (k_{calc}) and are compared with the measured k_{xy} in Table 4. As detailed in the notes to Table 4, the K_{eq} values are derived from the relevant BDFEs [except for the directly measured K_{eq} for $^{t}Bu_2(MeO)ArOH$], and the k_{yy} values are estimated from pseudo-self exchange reactions,

NIH-PA Author Manuscript

NIH-PA Author Manuscript

NIH-PA Author Manuscript

by application of the cross relation in other systems, or from values for related substrates. In applying eq 7, no correction has been made for the work required to assemble the [L_n V–OH···O=VL_n]$^{2+}$ precursor complex;[84] including the electrostatic component of this work ($w_r \cong +1.5$ kcal mol^{-1})[39,82,85] would raise the k_{calc} values by a factor of five. We estimate that the rate constants, k_{calc}, calculated from eq 7 have an uncertainty of 1–2 orders of magnitude, due to the uncertainties in the BDFEs, in the estimated substrate k_{yy} values, and in the work terms. The k_{calc} for the reaction of **2a** with ^{t}Bu$_2$(MeO)ArOH is more precise because the K_{eq} was measured directly rather than from BDFEs.

The calculated rate constants for transfer of a hydrogen atom are in fair agreement with the experimental values, with k_{xy}/k_{calc} varying from 0.05 to 80. While some of the values are outside the estimated errors, the cross relation captures the major trends in the rate constants for a range of organic substrates and for values of k_{xy} that range over almost six orders of magnitude. For example, the reaction of **2a** with DHA is ~10^5 times slower than reaction of **2a** with hydroquinone, at a similar driving force, because k_{yy} for DHA is much slower than that of hydroquinone.

The Marcus analysis indicates that the slow hydrogen transfer reactions of the vanadium compounds can be traced to the very slow $V^{IV}O(OH)^+/V^VO_2^+$ self-exchange rate constant. For example, **2a** oxidizes TEMPOH 10^4 times more slowly than Fe^{III}(Hbim)(H_2bim)$_2^{2+}$ (at the same driving force) because hydrogen-transfer self-exchange is much slower for vanadium than iron (H_2bim = 2,2′-biimidazoline). All of the slow rates reported here can largely be attributed to an unusually high intrinsic barrier for hydrogen atom self-exchange for $V^{IV}O$(OH)/V^VO_2. The origins of this high barrier for hydrogen atom self-exchange are discussed below.

IV. Computational Insights

As described above, DFT calculations at the B3LYP/6-31G(d) level, with a polarizable continuum solvent model appropriate for MeCN, give $\Delta H^‡$ of 12.4 kcal mol^{-1} for the **1c** + **2c** self-exchange reaction. This calculated value is in good agreement with the experimental activation enthalpy of 15 ± 2 kcal mol^{-1} for **1a** + **2b** in MeCN. This agreement supports the conclusion that this self-exchange reaction occurs by a concerted transfer of the electron and proton with a comparatively high enthalpic barrier. Since the calculations did not include any proton tunneling or non-adiabatic effects, the agreement also suggests that such effects are not of great importance in this reaction.

Computational studies have also examined the ruthenium oxo/hydroxo H-atom self-exchange reactions $Ru^{IV}O(L)(bpy)_2^+ + Ru^{III}OH(L)(bpy)_2^+$ for L = fluoride and pyrrolate (pyrr), as models for the experimentally studied dicationic compounds with L = pyridine.[28a] Starting from the hydrogen-bonded complexes, the calculated enthalpic barriers for RuO(pyrr) + Ru(OH)(pyrr) and RuO(F) + Ru(OH)(F) are 4.2 and 6.0 kcal mol^{-1} lower, respectively, than for **1c** + **2c**. These differences in activation enthalpies correspond to differences in rate constants of 10^3 and 10^4. Thus the majority of the experimentally observed 10^6 difference in self-exchange rates between the vanadium and ruthenium complexes is mirrored by our calculations.

A. Origin of the barriers—The difference in calculated electronic energies between the transition structures and hydrogen-bonded complexes is 5.8 kcal mol^{-1} larger for V than for Ru(O)F. The close correspondence between this $\Delta\Delta E^‡$ and the computed values of $\Delta\Delta H^‡$ = 6.0 kcal mol^{-1} (both in solution and in the gas-phase) has allowed us to understand the experimental difference between the self-exchange rates of the V and Ru complexes in solution by analyzing the origins of the differences between the electronic energies of the reactions in the gas-phase.

NIH-PA Author Manuscript

NIH-PA Author Manuscript

NIH-PA Author Manuscript

We have divided the passage from the optimized geometries of the hydrogen-bonded precursor complexes to the transition structures into three steps (**a** → **d** in Figure 8). First, the O···O distances in the hydrogen-bonded complexes (**a**) were shortened to those in the transition structures, but with all other geometrical parameters reoptimized (**b**). As can be seen in Figure 8 the energies required for this step are the same to within 1.0 kcal mol^{-1}, with the vanadium complex actually being the lowest. The similarity of these energy changes reflects the similar charge and steric environments around the metal oxo moieties in all three complexes.

In the next step (**b** → **c**), all of the atoms except for the transferring hydrogen were moved to their positions in the transition structures, and the positions of the transferring hydrogens were optimized. This step is 5.1 to 5.2 kcal mol^{-1} more difficult for the vanadium than for the ruthenium complexes, and thus accounts for almost all of the differences in activation energies between the V and Ru compounds. The final step of the cycle involves moving the proton to the symmetrical position that it occupies in the transition structures (**c** → **d**). Once again the energies required for this step are very similar among the three complexes, being only 1.2 kcal mol^{-1} more difficult for VO_2/VOOH than for RuO(F)/Ru(OH)(F).[89]

The results in Figure 8 show that the difference between the barrier heights in the vanadium and ruthenium systems arises predominantly from the differences between the energies that are required to change the M=O, M–OH, and M–N bonds from their lengths in the precursor complexes to their lengths in the transition structures. In the Marcus model, the energies associated with these changes are part of the inner-sphere reorganization energies, λ_i.

Single-point calculations were also performed on the isolated vanadium and ruthenium oxo and hydroxo species, in order to probe the energetic consequences of the bond length changes between the reactant and transition state structures.[39] Shortening the M–OH bond lengths of the hydroxo complexes, as occurs in the **b** → **c** step of Figure 8, is more energetically costly for $V(O)(OH)(bpy)_2^+$ (**1c**) than for $Ru(OH)(L)(bpy)_2^+$, by 2.3 and 2.7 kcal mol^{-1} for L = pyrr and F, respectively. Slightly larger energy differences are calculated for stretching the M=O bonds of the oxo compounds, 3.2 and 3.0 kcal mol^{-1} greater for **2c** than for the RuO(pyrr) and RuO(F) complexes. Together, these distortions are 5.5 – 5.7 kcal mol^{-1} more difficult for vanadium than for the ruthenium complexes, in good agreement with the calculated differences of 5.1 – 5.2 kcal mol^{-1} for step (**b**) to (**c**) in Figure 8. Thus, the difference in hydrogen exchange barriers, both observed and calculated, can be traced to the greater energetic cost for vanadium than for ruthenium of changing the M=O and M-OH bonds from their lengths in the hydrogen-bonded reactant complexes to their lengths in the transition structures for the self-exchange reactions.

Figure 9 provides the M–OH and M=O bond lengths in the reactants, hydrogen-bonded complexes, and transition structures. The M–OH and M=O bonds are calculated to be 0.1–0.2 Å shorter for M = V than for M = Ru, as expected.[90,91] In going from the reactants or the hydrogen-bonded complexes to the transition structures, the *changes* in M–OH and M=O bond lengths are larger for vanadium than for ruthenium. The M–OH bonds contract by *ca*. 0.05 Å more for V and the M=O bonds lengthen by *ca*. 0.04 Å more for V. In addition, the shorter V–OH and V=O bonds have higher force constants. For example, the experimental frequency of the symmetric VO_2 stretch is 927 cm^{-1} in **2a***vs*. ν(Ru=O) = 800 cm^{-1} in $Ru^{IV}O(L)(bpy)_2^+$.[40,92] The calculated frequencies are $\nu_{symm}(VO_2)$ = 1060 cm^{-1} in **2c** and ν(Ru=O) = 795 and 798 cm^{-1} for, respectively, RuO(pyrr) and RuO(F). Therefore, the reorganization energies are higher in the vanadium complexes than in the ruthenium complexes for two reasons -- larger changes in M–OH and M=O bond lengths are required to reach the transition structure for M = V than for M = Ru, and these larger changes are magnified by the higher force constants for the V–O and V=O bonds.

NIH-PA Author Manuscript

NIH-PA Author Manuscript

NIH-PA Author Manuscript

The metal-oxygen bond-length distortion energies for moving from the reactant to the transition structure are computed to be greater in the vanadium vs. the ruthenium reactions. This is a consequence of the structure of the reactants: the 0.264 Å difference between the V–OH and V=O bond lengths is *ca*. 0.10 Å larger than 0.167 – 0.168 Å difference between the Ru–OH and Ru=O bond lengths. Therefore, the key to understanding the greater reorganization energy in the self-exchange reaction of the vanadium versus the ruthenium complexes is understanding why the difference between the M–OH and M=O bond lengths is 50% larger for V than for Ru.

B. Differences between the Reductions of $(bpy)_2VO_2^+$ (2c) and $(bpy)_2RuOX^+$—

The larger M=O ➔ M-OH bond length change for M = V than for M = Ru can be understood in terms the differences between the electronic structures of the vanadium and ruthenium reactants and, in particular, the different d-orbital occupancies in these complexes. The vanadium-dioxo compounds **2a–c** have a total of three formal metal-oxo π bonds. Two of these bonds come from electron donation from the filled $2p_\pi$ atomic orbital (AO) on each oxygen that is perpendicular to the O-V-O plane into an empty t_{2g} orbital on the d^0 vanadium(V) cation. The third π bond consists of two partial π bonds, involving donation from the filled $2p_\pi$AO on each oxygen that lies in the O-V-O plane, into the third empty t_{2g} orbital, on the d^0 vanadium (V) cation.[41]

Addition of H• ($e^- + H^+$) to one of the oxygen atoms in **2a–c** causes dramatic changes in π bonding. The added electron goes into the V–O π* orbital that is of δ symmetry relative to the remaining V=O bond (as is typical of $[L_nV^{IV}(O)]$ complexes[18a,41,42,72a]). The π bonding between the vanadium center and the hydroxide ligand is quite weak, as indicated by calculations of the calculated changes in V–O bond distance and spin densities as a function of the O-V-O-H dihedral angle (see Supporting Information). Complex **1c** is well-described as having a V≡O triple bond to the oxo oxygen and a V–O single bond to the hydroxyl group. Formation of **1c** by transfer of a hydrogen atom to **2c** therefore results in the formal loss of a full V-O π bond.

In contrast, reduction of $Ru^{IV}(O)L(bpy)2^+$ complexes results in the loss of only half a π bond. Unlike V^V dioxo complexes such as **2c**, which have no 3d electrons, ruthenium(IV)–mono-oxo compounds have four electrons in the Ru t_{2g} 4d AOs. Two of these electrons occupy Ru–O π* orbitals.[41,91d] These complexes therefore have only two half π bonds. Although the total Ru–O π bond order is formally one, each of these half π bonds is expected to be weak.[93]

Addition of H• to the ruthenium oxo group lowers the formal Ru-O π bond order to 0.5. In $Ru(OH)F^+$, the remaining unpaired electron preferentially occupies a 4d AO that lies in the F-Ru-O plane. A scan of the F-Ru-O-H dihedral angle (see Figure S13 and the accompanying text in the Supporting Information) finds that the global minimum occurs at F-Ru-O-H = 99.8°, where the lone pairs in $2p_\pi$ AOs on both F and OH can interact with this singly occupied 4d AO. The scan shows two maxima, at F-Ru-O-H = 357.6° and 232.4°, and a secondary minimum, at F-Ru-O-H = 232.4°. The averaged maxima are 6.9 kcal mol^{-1} higher in energy than the averaged minima, and have 0.34 Å longer Ru-OH bond lengths. These results indicate that, unlike the case in the vanadium complex **1c**, there is a significant, albeit weak, π bond to the OH group in Ru(OH)F. Consistent with this conclusion is the finding that, at the equilibrium geometry of Ru(OH)F, 17.0% of the unpaired spin is localized on the hydroxyl group; whereas, in **1c**, only 3.1 % of the unpaired spin appears on the hydroxyl group.

In summary, the calculations provide a detailed understanding of the differences in the heights of the barriers to hydrogen atom self-exchange in the vanadium and ruthenium systems. As illustrated in Figure 10, addition of H• to **2** decreases the π bond order for one V–O bond from 1.5 to close to 0, while the other V–O increases its π bond order from 1.5 to 2. In contrast,

NIH-PA Author Manuscript

NIH-PA Author Manuscript

NIH-PA Author Manuscript

addition of H• to the $Ru^{IV}(O)X$ complexes results in a bond order decrease of only *ca*. 0.5 of a weak π bond. The larger changes in π bond order upon hydrogen atom addition to **2** than to $Ru^{IV}(O)X^{+}$ are reflected in larger changes in M–O bond lengths, both observed and computed, for the vanadium than the ruthenium complexes. These larger changes in M-O bond lengths on H• addition to **2**, compounded by the higher force constants for the V–O bonds, are the origin of the larger inner-sphere reorganization energies for hydrogen self-exchange in the vanadium vs. the ruthenium complexes.

C. The nature of the e^{-}/H^{+} transfer: PCET *vs.* HAT—Traditionally, any reaction that involved net transfer of H• from one reagent to another (eq 5 above) has been termed hydrogen atom transfer or HAT. Some years ago, Meyer proposed that HAT should be restricted to processes where "the transferring electron and proton come from the same bond." [1,94] More recently, some of us showed that H• self-exchange between phenoxyl radical and phenol does not resemble HAT, but rather involves proton transfer between two oxygen lone pairs coupled to electron transfer between phenoxyl π orbitals.[95] We termed this mechanism proton-coupled electron transfer (PCET) to distinguish it from HAT, and others have found this distinction useful.[71] Unfortunately, PCET now has a much broader usage, often referring to any electron transfer process whose overall rate is affected by proton(s). Truhlar and coworkers have recently proposed an alternative distinction between HAT and PCET processes.[96]

Using the original definition of PCET, the vanadium self-exchange reaction is a PCET process, not HAT. There is concerted transfer of $e^{-} + H^{+}$ in which the electron is not associated with the VO–H bond. This is shown by the nature of the SOMO at the transition structure (Figure 11). The SOMO is V–OH π antibonding and is, at each vanadium, orthogonal to the O–H bond that is being made or broken. This is the clear indication of a PCET pathway.

Analysis of the ruthenium self-exchange reactions is more complicated because there are three half-filled orbitals at the transition structure (Figure S14). One of these SOMOs resembles the vanadium PCET SOMO but another resembles the SOMO at a classical HAT transition structure. This illustrates a difficulty with the PCET/HAT dichotomy. Only in favorable cases can this distinction be made, even in the simplest case of self-exchange reactions. In cross reactions, the situation is often much more complicated. In the reactions of **2a** with xanthene and dihydroanthracene, for instance, the mechanism is PCET from the perspective of the vanadium center but HAT from the perspective of the C–H bond. In many cases it can be quite challenging to make a PCET/HAT distinction in the absence of detailed calculations. Therefore we favor using the term HAT in its traditional way, to "refer to what is *transferred* between reactants in the net sense and *not to the mechanism* of the event,"[97] unless the context makes clear that a detailed orbital picture is implied.

Conclusions

Reactions that interconvert dioxo-vanadium(V) compounds $[V^{V}O_2(R_2bpy)_2]BF_4$ (R = ^{t}Bu, Me, H) (**2a–c**) and oxo-hydroxo-vanadium(IV) compounds $[V^{IV}O(OH)(R_2bpy)_2]BF_4$ (**1a–c**) [18] have been examined. Together, these compounds comprise a system of sterically uncrowded and isolable metal-oxo and metal-hydroxo compounds that differ only by a hydrogen atom ($H^{+} + e^{-}$). Compound **2a** abstracts a hydrogen atom from 2,6-$^{t}Bu_2$-4-MeO-C_6H_2OH (ArOH), TEMPOH, dihydroanthracene, xanthene, and hydroquinone, while 2,4,6-$^{t}Bu_3C_6H_2O$• abstracts H• from **1a**. The reaction of **2a** with ArOH reaches a measurable equilibrium, indicating that the VO–H bond dissociation free energy (BDFE) in **1a** is 70.6 kcal mol^{-1}. The reactions of **2a** with hydrogen atom donors are all surprisingly slow, with second order rate constants from 1×10^{-1} M^{-1} s^{-1} to 2×10^{-7} M^{-1} s^{-1}. Hydrogen atom pseudo-self-exchange between $V^{IV}O(OH)(R_2bpy)_2^{+}$ and $V^{V}O_2(R'_2bpy)_2^{+}$ (R, R′ = ^{t}Bu, Me) is also surprisingly slow, with $k_{se} = 1.3 \times 10^{2}$ M^{-1} s^{-1} at 298 K. This is 6×10^{6} slower than the self-exchange rate constant

NIH-PA Author Manuscript

NIH-PA Author Manuscript

NIH-PA Author Manuscript

measured for the sterically similar $Ru^{IV}(O)(py)bpy_2^{2+}$ + $Ru^{III}(OH)(py)bpy_2^{2+}$.[27e] The activation parameters for vanadium self-exchange, $\Delta H^{\ddagger} = 15 \pm 2$ kcal mol^{-1} and $\Delta S^{\ddagger} = -16 \pm 5$ cal mol^{-1} K^{-1} ($A = 4 \times 10^9$ s^{-1}), suggest that this is an adiabatic reaction with a relatively large barrier. Using the vanadium self-exchange rate constant, the Marcus cross relation predicts the rate constants of the HAT cross rates within two orders of magnitude in most cases.

DFT calculations of the vanadium self-exchange reaction **1c** + **2c**, using a PCM solvent model, give a calculated barrier height of $\Delta H^{\ddagger} = 12.4$ kcal mol^{-1} above the separated reactants and 17.1 kcal mol^{-1} above the hydrogen-bonded precursor complex $[(bpy)_2(O)V–OH \cdots O=V(O)–(bpy)_2]^{2+}$. Passage to the transition structure involves large changes in the V–O bond lengths. These distortions are larger than the corresponding bond length changes in model ruthenium complexes $Ru^{IV}(O)(X)bpy_2^{+}$/$Ru^{III}(O)(X)bpy_2^{+}$ (X = F$^-$, pyrrolate). The difference between the vanadium and ruthenium complexes is due to a larger change in the net π bond order in the former than in the latter, which can, in turn, be traced to the differing d-orbital occupancies of the V *vs*. Ru complexes. The larger bond length distortions and higher force constants make the Marcus inner sphere reorganization energy, λ_i, larger for the vanadium than for the ruthenium reactions, leading to the dramatic 10^6 difference in reactivity.

We have previously emphasized the importance of driving force in understanding hydrogen atom transfer reactivity. This study emphasizes that differences in intrinsic barriers heights can have a dramatic effect as well.

Experimental Section

Reagent grade chemicals and solvents were obtained from Aldrich, Eastman Organic, Strem, Fisher Scientific or EMD Chemicals and used without further purification unless otherwise noted. CH_2Cl_2 was dried using a “Grubbs type” Seca Solvent System installed by GlassContour.[98] MeCN (Burdick and Jackson low water brand) was stored in an argon-pressurized steel drum plumbed directly into a glovebox. Deuterated solvents were purchased from Cambridge Isotope Laboratories. CD_2Cl_2 was dried by stirring over CaH_2 followed by vacuum transfer and stored in a dark bottle in a glovebox freezer. CD_3CN was dried over CaH_2, vacuum transferred to P_2O_5 for 30 min, then CaH_2 again, and transferred to a clean flask and stored in a glovebox. TEMPOH[29] and $^tBu_3PhO\bullet$[53] were prepared following literature procedures. $^tBu_3PhOH$ and $^tBu_2(MeO)PhOH$ were recrystallized twice from hexanes or ethanol, respectively. Hydroquinone was recrystallized from MeCN.

The vanadium compounds were synthesized under air, dried *in vacuo*, and stored in a N_2 glovebox. All other reactions were performed under N_2 using standard glovebox and Schlenk techniques, often in sealable (J-Young) NMR tubes or quartz cuvettes fitted with Teflon stopcock. ^{1}H and ^{13}C NMR spectra were recorded on Bruker Avance or DRX spectrometers (300 and 500 MHz) at ambient temperatures unless otherwise noted and are referenced to a solvent peak. Electrospray ionization mass spectra (ESI/MS) were obtained on a Bruker Esquire-LC ion trap mass spectrometer as solutions in acetonitrile. IR spectra were recorded as KBr pellets or CH_2Cl_2 solutions in a cell with NaCl windows (as noted) using either a Perkin-Elmer 1720 or a Bruker Vector 33 FT-IR spectrometer and are reported in cm^{-1}. UV-vis spectra were recorded using a Hewlett-Packard 8453 spectrometer and are reported as λ in nm (Σ, M^{-1} cm^{-1}). Experimental details for the X-ray structure of **2c** are given in the Supporting Information.

Syntheses

The preparations of the $^tBu_2$bpy derivatives are given here; the similar procedures for the Me_2bpy and bpy complexes are given in the Supporting Information.

NIH-PA Author Manuscript

NIH-PA Author Manuscript

NIH-PA Author Manuscript

cis-[$V^{IV}O(OH)(4,4'$-^{t}Bu$_2$bpy)$_2$]BF_4 (1a)

In a simpler procedure than the literature method,[18b] aqueous HBF_4 (48 wt %, ~0.3 mL, 2.3 mmol) was added to a solution of $V(O)SO_4$•$2(H_2O)$ (260 mg, 1.33 mmol) in 2 mL deionized H_2O, to make the pH 1.0 (by pH meter). $BaCO_3$ (0.270 g, 1.36 mmol) was added, evolution of CO_2 was observed, and the white precipitate ($BaSO_4$) was removed by filtration through Celite. Upon addition of ^{t}Bu$_2$bpy (870 mg, 3.24 mmol), the clear blue solution changed to red-brown and a yellow precipitate formed. Stirring for 2 h and filtration gave a light yellow solid, which was washed with Et_2O and dried *in vacuo* to give 752 mg (80%) of **1a**. Crystals of **1a** were obtained by slow evaporation of a CH_2Cl_2/toluene (1:1 v/v) solution. ^{1}H NMR (CD_3CN): δ 1.365, 1.584 1.672, 2.705 (br, ^{t}Bu, 9H each). IR (KBr pellet): 969 cm^{-1} vs ν(V=O), 1615 vs ν(C=C, C=N), 2961 vs ν(C–H). UV-Vis (CH_3CN): 753 (26), 521 (37), 301 (24620), 261 (11875). ESI/MS (CH_3CN): 622 [**1a** + 2H - BF_4]$^+$, 619 [**1a**]$^+$.

cis-[$V^{V}O_2(4,4'$-^{t}Bu$_2$bpy)$_2$]BF_4 (2a)

^{t}Bu$_2$bpy (2.4 g, 8.96 mmol) was added to a solution of $NaVO_3$ (0.546 g, 4.48 mmol) in 75 mL aqueous HBF_4 (pH = 1). Stirring overnight yielded a pale yellow precipitate, which was collected by filtration. The precipitate was dissolved in CH_2Cl_2 and the solution was washed three times with aqueous $NaHCO_3$, then with water. The volume was reduced to ~20 mL and 200 mL pentane added dropwise to give a fine yellow precipitate that was collected by filtration and dried *in vacuo* (2.812 g, 89% yield). Anal. Calcd for **2a**•½CH_2Cl_2 (CH_2C1_2 was observed in these samples by NMR), $C_{36.5}H_{49}BC1F_4N_4O_2V$: C, 58.53; H, 6.59; N, 7.48. Found: C, 58.7; H, 6.61; N, 7.48. ^{1}H NMR ($CD_2C1_2$205 K): ^{t}Bupy *A*: δ1.28 (s, ^{t}Bu, 18H); 7.34 (4H, 6-bpy and 5-bpy); 8.13 (s, 2H, 3-bpy); ^{t}Bupy *B*: 1.46 (s, ^{t}Bu, 18H); 7.73 (d, 5.5 Hz, 2H, 5′-bpy H); 8.29 (s, 2H, 3′-bpy H); 8.91 (d, 5.5 Hz, 2H, 6′-bpy H). ^{13}C{^{1}H} NMR (CD_2C1_2 205 K): δ29.65, 29.71 (C(CH_3)$_3$); 36.39, 36.03 (*C*Me$_3$); 119.72, 119.85, 124.84 (2C), 146.48, 149.35, 153.40, 156.06, 156.06, 164.63, 168.21 (bpy). At 298 K in CD_2C1_2 or CD_3CN, one broad ^{l}Bu peak is observed at 1.4 ppm and three very broad bpy peaks are observed at 7.5, 8.3 and 8.9 ppm. ESI/MS (CH_3CN): *m*/*z* 619 [**2a** - BF_4]$^+$, 87 [BF_4]$^-$ IR (CH_2C1_2 soln): 927, 906 s ν(V=0), 1618, 1546 vs ν(C=C, C=N), 2973 s ν(C-H). UV-Vis: (CH_3CN) 305 (20,000).

Pseudo Self-Exchange Experiments

In a typical experiment, a septum-sealed NMR tube in a N_2 glovebox was charged with **2a** (500 μL, 17 mM in CD_3CN) and ($Me_3Si)_2O$ (~lμL) as an internal standard. A gastight syringe was loaded with 300 μL of a solution of **lb** (8 mM in CD_3CN). The syringe and NMR tube were then removed from the glovebox and the NMR tube frozen in liquid nitrogen. The contents of the syringe were then added to the NMR tube, which was thawed immediately before inserting into the NMR which was pre-equilibrated at the desired temperature. Spectra were recorded until equilibrium was reached. Reactions starting with solutions of **la** and **2b** were also performed.

The reaction of 2a + ArOH

was monitored by optical spectroscopy (350 – 900 nm). Concentrations at equilibrium were calculated using the known spectra of **la** and ArO• in MeCN and assuming mass balance according to equation 4. The kinetics were analyzed using SPECFIT[52] with a second-order approach to equilibrium model; the vanadium spectra and K_4 were fixed. The calculated spectra of ArO• were in good agreement with experiment. Initial concentrations were varied from 1.1 – 23 mM **(2a)** and 3 – 300 mM (ArOH).[39]**The kinetics of 2a + xanthene** were measured using 5 to 20 equivalents of xanthene, and modeled as a second order process in SPECFIT with the spectrum of **la** fixed.

NIH-PA Author Manuscript

NIH-PA Author Manuscript

NIH-PA Author Manuscript

Solutions of 2,6-$^{t}Bu_2$-4-(MeO)C_6H_2O• (ArO•)

were generated via oxidation of ArOH with NaOH and $K_3[Fe^{III}(CN)_6]$ in a biphasic benzene/water mixture.[53] The resulting 0.2 M solution in C_6H_6 contained ~ 0.1 to 0.2 M phenol impurities, including ArOH. Extinction coefficients were measured by titrating solutions of ArO• with known amounts of TEMPOH. UV-Vis: 535 (230), 405 (4000), 389 (2800), 336 (5800). The λ_{max} values are consistent with those reported by Modarelli *et al.* in pentane, [99] but the molar absorptivities measured here are larger.

Supplementary Material

Refer to Web version on PubMed Central for supplementary material.

Acknowledgement

We thank the U.S. National Institutes of Health (GM50422) and the University of Washington for financial support to JMM, and the National Science Foundation and Robert A. Welch Foundations for support to WTB. We also thank Dr. Martin Sadilek for assistance with mass spectrometry.

References

1. Huynh MHV, Meyer TJ. Chem. Rev 2007;107:5004–5064. [PubMed: 17999556]
2. Meyer TJ, Huynh MHV. Inorg. Chem 2003;42:8140–8160. [PubMed: 14658865]
3. Stubbe J, Nocera DG, Yee CS, Chang MCY. Chem. Rev 2003;103:2167. [PubMed: 12797828]
4. Mayer JM. Ann. Rev. Phys. Chem 2004;55:363–390. [PubMed: 15117257]
5. Mayer JM, Rhile IJ. Biochim. Biophys. Acta 2003:51–58.
6. Costentin C, Evans DH, Robert M, Savéant J-M, Singh PS. J. Am. Chem. Soc 2005;127:12490–12491. [PubMed: 16144387]
7. (a) Rhile IJ, Markle TF, Nagao H, DiPasquale AG, Lam OP, Lockwood MA, Rotter K, Mayer JM. J. Am. Chem. Soc 2006;128:6075–6088. [PubMed: 16669677] (b) Markle TF, DiPasquale AG, Mayer JM. Angew. Chem. Int. Ed 2008;47:738–740. (c) Markle TF, DiPasquale AG, Mayer JM. Proc. Natl. Acad. Sci 2008;105:8185–8190. [PubMed: 18212121]
8. Meunier B, Visser SP, Shaik S. Chem. Rev 2004;104:3947–3980. [PubMed: 15352783]
9. (a) Riggs-Gelasco PJ, Price JC, Guyer RB, Brehm JH, Barr EW, Bollinger JM Jr, Krebs C. J. Am. Chem. Soc 2004;126:8108–8109. [PubMed: 15225039] (b) Price JC, Barr EW, Hoffart LM, Krebs C, Bollinger JM Jr. Biochemistry 2005;44:8138–8147. [PubMed: 15924433] (c) Krebs C, Fujimori DC, Walsh CT, Bollinger JM Jr. Acc. Chem. Res 2007;40:484–492. [PubMed: 17542550]
10. (a) Baik M, Newcomb M, Friesner RA, Lippard SJ. Chem. Rev 2003;103:2385–2419. [PubMed: 12797835] (b) Gherman BF, Lippard SJ, Friesner RA. J. Am. Chem. Soc 2004;127:1025–1037. [PubMed: 15656641]
11. Stubbe J, van der Donk WA. Chem. Rev 1998;98:705–762. [PubMed: 11848913]
12. (a) Limberg C. Angew. Chem. Int. Ed 2003;42:5932–5954. (b) Coulston GW, Bare SR, Kung H, Birkeland K, Bethke GK, Harlow R, Herron N, Lee PL. Science 1997;275:191–193. [PubMed: 8985008] (c) Centi G, Trifiro F, Ebner JR, Franchetti VM. Chem. Rev 1988;88:55–80.
13. Mijs WJ, Jonge CRHI. Organic Synthesis by Oxidation with Metal Compounds. 1986New YorkPlenum Press (b) See also references 27.
14. Pourbaix, M. Atlas of Electrochemical Equilibria in Aqueous Solutions. New York: Pergamon Press; 1966. p. 365Baes, CF., Jr; Mesmer, RE. The Hydrolysis of Cations. New York: Wiley; 1976. Richens, DT. The Chemistry of Aqua Ions. New York: Wiley; 1997. Stumm, W.; Morgan, JJ. Aquatic Chemistry. New York: Wiley; 1996.
15. (a) References 1, 2. (b)Lebeau EL, Binstead RA, Meyer TJ. J. Am. Chem. Soc 2001;123:10535. [PubMed: 11673985] (c)Hurst JK, Cape JL, Clark AE, Das S, Qin C. Inorg. Chem 2008;47:1753–1764.1764 [PubMed: 18330967] (d)Cape JL, Hurst JK. J. Am. Chem. Soc 2007;130:827–829.829 [PubMed: 18161977] (e)Farrer BT, Thorp HH. Inorg. Chem 1999;38:2497–2502.2502 (f)Muller JG, Acquaye JH, Takeuchi KJ. Inorg. Chem 1992;31:4552–4557.4557 (g)Lam WWY, Man W-L, Lau

NIH-PA Author Manuscript

NIH-PA Author Manuscript

NIH-PA Author Manuscript

T-C. Coord. Chem. Rev 2007;251:2238–2252.2252 (h)Romero I, Rodríguez M, Sens C, Mola J, Rao Kollipara M, Francàs L, Mas-Marza E, Escriche L, Llobet A. Inorg. Chem 2008;47:1824–1834.1834 [PubMed: 18330973] (i)Masllorens E, Rodriguez M, Romero I, Roglans A, Parella T, Benet-Buchholz J, Poyatos M, Llobet A. J. Am. Chem. Soc 2006;128:5306–5307.5307 [PubMed: 16620078]

16. (a) Bakac A. J. Am. Chem. Soc 2000;122:1092–1097. (b) Vasbinder MJ, Bakac A. Inorg. Chem 2007;46:2921–2928. [PubMed: 17290988] (c) Pestovsky O, Bakac A. J. Am. Chem. Soc 2004;126:13757–13764. [PubMed: 15493935]
17. (a) Gupta R, MacBeth CE, Young VG Jr, Borovik AS. J. Am. Chem. Soc 2002;124:1136–1137. [PubMed: 11841259] (b) Parsell TH, Behan RK, Green MT, Hendrich MP, Borovik AS. J. Am. Chem. Soc 2006;128:8728–8729. [PubMed: 16819856] (c) Gupta R, Borovik AS. J. Am. Chem. Soc 2003;125:13234–13242. [PubMed: 14570499] (d) Qin K, Incarvito CD, Rheingold AL, Theopold KH. J. Am. Chem. Soc 2002;124:14008–14009. [PubMed: 12440895] (e) Van Kirk CC, Qin K, Theopold KH, Evans DH. J. Electroanal. Chem 2004;565:185–190.
18. (a) Tolis EJ, Manos MJ, Raptopoulou CP, Terzis A, Sigalas MP, Deligiannakis Y, Kabanos TA. Angew. Chem. Int. Ed 2002;41:2797–2800. (b) Triantafillou GD, Tolis EI, Terzis A, Deligiannakis Y, Raptopoulou CP, Sigalas MP, Kabanos TA. Inorg. Chem 2004;43:79–91. [PubMed: 14704056]
19. (a) Brand SG, Edelstein N, Hawkins CJ, Shalimoff G, Snow MR, Tiekink ERT. Inorg. Chem 1990;29:434–438. (b) Qi Y, Yang Y, Cao M, Hu C, Wang E, Hu N, Jia H. J. Mol. Struct 2003;648:191–201.
20. (a) Crans DC, Smee JJ, Gaidamauskas E, Yang L. Chem. Rev 2004;104:849–902. [PubMed: 14871144] (b) Rehder D, Santoni G, Licini GM, Schulzke C, Meier B. Coord. Chem. Rev 2003;237:53–63. (c) Kanamori K, Nishida K, Miyata N, Okamoto K, Miyoshi Y, Tamura A, Sakurai H. J. Inorg. Biochem 2001;86:649–656. [PubMed: 11583782]
21. (a) Butler AJ. Curr. Opin. Chem. Biol 1998;2:279–285. [PubMed: 9667930] (b) Butler AJ. Coord. Chem. Rev 1999;187:17–35.
22. Hirao T. Chem. Rev 1997;97:2707–2724. [PubMed: 11851478]
23. Kobayashi H, Yamanaka I. Chem. Lett 2007;36:114–115.
24. Butler AJ, Clague MJ, Meister GE. Chem. Rev 1994;94:625–638.
25. (a) Chen K, Khodakov A, Yang J, Bell AT, Iglesia E. J. Catal 1999;186:325–333. (b) Chen K, Bell AT, Iglesia E. J. Phys. Chem. B 2000;104:1292–1299.
26. Bregeault J, Veannat M, Salles L, Piquemal J, Mahha Y, Briot E, Bakala PC, Atlamsani A, Thouvenot R. J. Mol. Catal. A 2006;250:177–189.
27. (a) Mayer JM. Acc. Chem. Res 1998;31:441–450. (b) Cook GK, Mayer JM. J. Am. Chem. Soc 1994;116:1855. (c) Cook GK, Mayer JM. J. Am. Chem. Soc 1995;117:7139–7156. (d) Gardner KA, Mayer JM. Science 1995;269:1849. [PubMed: 7569922] (e) Gardner KA, Kuehnert LL, Mayer JM. Inorg. Chem 1997;36:2069. [PubMed: 11669825]
28. (a) Bryant JR, Mayer JM. J. Am. Chem. Soc 2003;125:10351–10361. [PubMed: 12926960] (b) Bryant JR, Mayer JM. Inorg. Chem 2004;43:1587–1592. [PubMed: 14966998]
29. (a) Mader EA, Larsen AS, Mayer JM. J. Am. Chem. Soc 2004;126:8066–8067. [PubMed: 15225018] (b) Mader EA, Davidson ER, Mayer JM. J. Am. Chem. Soc 2007;129:5153–5166. [PubMed: 17402735]
30. Roth JP, Yoder JC, Won T, Mayer JM. Science 2001;294:2524–2526. [PubMed: 11752572]
31. Soper JD, Mayer JM. J. Am. Chem. Soc 2003;125:12217–12229. [PubMed: 14519007]
32. (a) Warren JJ, Mayer JM. J. Am. Chem. Soc 2008;130:2774–2776. [PubMed: 18257574] (b) Manner VW, DiPasquale AG, Mayer JM. J. Am. Chem. Soc 2008;130:7210–7211. [PubMed: 18479096]
33. (a) Goldsmith CR, Jonas RT, Stack TDP. J. Am. Chem. Soc 2001;124:83–96. [PubMed: 11772065] (b) Goldsmith CR, Cole AP, Stack TDP. J. Am. Chem. Soc 2005;127:9904–9912. [PubMed: 15998097] (c) Goldsmith CR, Stack TDP. Inorg. Chem 2006;45:6048–6055. [PubMed: 16842013]
34. (a) Groves JT, Subramanian DV. J. Am. Chem. Soc 1984;106:2177–2181. (b) Lansky DE, Goldberg DP. Inorg. Chem 2006;45:5119–5125. [PubMed: 16780334] (c) Goldberg DP. Acc. Chem. Res 2007;40:626–634. [PubMed: 17580977] (d) Itoh S, Bandoh H, Nakagawa M, Nagatomo S, Kitagawa T, Karlin KD, Fukuzumi S. J. Am. Chem. Soc 2001;123:11168–11178. [PubMed: 11697960] (e) Taki M, Itoh S, Fukuzumi S. J. Am. Chem. Soc 2001;123:6203–6204. [PubMed: 11414865] (f) Leung

NIH-PA Author Manuscript

NIH-PA Author Manuscript

NIH-PA Author Manuscript

SK-Y, Tsui W-M, Huang J-S, Che C-M, Liang J-L, Zhu N. J. Am. Chem. Soc 2005;127:16629–16640. [PubMed: 16305252]

35. (a) Lewis EA, Tolman WB. Chem. Rev 2004;104:1047–1076. [PubMed: 14871149] (b) Cramer CJ, Tolman WB. Acc. Chem Res 2007;40:601–608. [PubMed: 17458929] (c) Tolman WB. Acc. Chem. Res 1997;30:227–237. (d) Pratt RC, Stack TDP. Inorg. Chem 2005;44:2367–2375. [PubMed: 15792472] (e) Mahadevan V, Henson MJ, Solomon EI, Stack TDP. J. Am. Chem. Soc 2000;122:10249–10250. (f) Obias HV, Lin Y, Murthy NN, Pidcock E, Solomon EI, Ralle M, Blackburn NJ, Neuhold Y, Zuberbühler AD, Karlin KD. J. Am. Chem. Soc 1998;120:12960–12961. (g) Shearer J, Zhang CX, Zakharov LN, Rheingold AL, Karlin KD. J. Am. Chem. Soc. 2005;127:5469–5483. (h) Mirica LM, Rudd DJ, Vance MA, Solomon EI, Hodgson KO, Heddman B, Stack TDP. J. Am. Chem. Soc 2006;128:2654–2665. [PubMed: 16492052]
36. (a) Sastri CV, Lee J, Oh K, Lee YJ, Lee J, Jackson TA, Ray K, Hirao H, Sin W, Halfen JA, Kim J, Que L Jr, Shaik S, Nam W. Proc. Natl. Acad. Sci. USA 2007:1–6. (b) Paine TK, Costas M, Kaizer J, Que L Jr. J. Biol. Inorg. Chem 2006:272–276. [PubMed: 16532334] (c) Bukowski MR, Koehntop KD, Stubna A, Bominaar EL, Halfen JA, Muenk E, Nam W, Que L Jr. Science 2005;310:1000–1002. [PubMed: 16254150] (d) Oh NY, Suh y, Park MJ, Seo MS, Kim J, Nam W. Angew. Chem. Int. Ed 2005;44(27):4235–4239.
37. (a) Lam WY, Man W, Leung C, Wong C, Lau T. J. Am. Chem. Soc 2007;129:13646–13652. [PubMed: 17929922] (b) Lam WWY, Yiu S, Lee JMN, Yau SKY, Kwong H, Lau T, Liu D, Lin Z. J. Am. Chem. Soc 2006;128:2851–2858. [PubMed: 16506763] (c) Lam WWY, Yiu S, Yiu DTY, Lau T, Yip W, Che C. Inorg. Chem 2003;42:8011–8018. [PubMed: 14632520] (d) Yiu DTY, Lee MFW, Lam WWY, Lau T. Inorg. Chem 2003;42:1225–1232. [PubMed: 12588160]
38. Waidmann CR, Mayer JM. manuscript in preparation.
39. See Supporting Information.
40. Tajika Y, Tsuge K, Sasaki Y. J. Chem. Soc., Dalton Trans 2005:1438–1447.
41. Nugent, WA.; Mayer, JM. Metal-Ligand Multiple Bonds. New York: Wiley and Sons; 1998. Chapters 2, 4 & 5.
42. Ballhausen CJ, Gray HB. Inorg. Chem 1962;1:111–122.
43. Kramarz, KW.; Norton, JR. Progress in Inorganic Chemistry. Karlin, KD., editor. Vol. 42. New York: John Wiley and Sons; 1994. p. 1-65. (b) Erikson TKG, Mayer JM. Angew. Chem. Int. Ed. Eng 1988;27:1527–1529.
44. (a) Bond MR, Czernuszewicz RS, Dave BC, Yan Q, Mohan M, Verastegue R, Carrano CJ. Inorg. Chem 1995;34:5857–5869. (b) Heater SJ, Carrano MW, Rains D, Walter RB, Ji D, Yan Q, Czernuszewicz RS, Carrano CJ. Inorg. Chem 2000;39:3881–3889. [PubMed: 11196784]
45. Czernuszewicz, RS.; Spiro, TG. Inorganic Electronic Structure and Spectroscopy. Solomon, EI.; Lever, ABP., editors. Vol. Vol. 1. New York: Wiley-Interscience; 1999. p. 353-442.
46. (a) See references 28–31, 70 and: (b)Wu A, Mayer JM. J. Am. Chem. Soc 2008;130:14745–14754.14754 [PubMed: 18841973] (c)Yoder JC, Roth JP, Gussenhoven EM, Larsen AS, Mayer JM. J. Am. Chem. Soc 2003;125:2629–2640.2640 [PubMed: 12603151]
47. MestReC. version 4.9.9.9, MestreLab Research SL.
48. (a) Pladziewicz JR, Lesniak JS, Abrahamson AJ. J. Chem. Educ 1986;63:850–851. (b) King EL. Int. J. Chem. Kinet 1982;14:1285–1286.
49. Because of the fluxional ^{1}H NMR spectra of **2a** and **2b**, rates can only be measured above 310 K (where the lines are sharper)or below 280 (where the peaks are decoalesced). Above 330 K, the reactions become too fast to measure by NMR.
50. (a) Altwicker ER. Chem. Rev 1967;67:475–531. (b) Cook CD, Kuhn DA, Fianu P. J. Am. Chem. Soc 1956;78:2002–2005.
51. The following references report BDE difference between ^{t}Bu$_3$PhOH and ^{t}Bu$_2$(MeO)ArOH: (a) Jackson RA, Hosseini KM. J.Chem. Soc., Chem. Commun 1992:785–787.787 (b)Lucarini M, Pedulli GF. J. Org. Chem 1994;59:5063–5070.5070 (c)Zhang X, Bordwell FG. J. Am. Chem. Soc 1994;116:4251–4254.4254 (d)Lucarini M, Pedrielli P, Pedulli GF. J. Org. Chem 1996;61:9259–9263.9263 The average ΔBDE is 3.1 ± 0.4 kcal mol^{-1}, assuming that the ΔBDFE is equal to the ΔBDE gives a BDFE of ^{t}Bu$_2$MeOPhOH of 73.9 kcal mol^{-1}.
52. SPECFIT/32, version v3.0.39b. Spectrum Software Associates: Marbourough, MA. 2000

NIH-PA Author Manuscript

NIH-PA Author Manuscript

NIH-PA Author Manuscript

53. Manner VW, Markle TF, Freudenthal JH, Mayer JM. Chem. Comm 2008:256–258. [PubMed: 18092105]
54. BDFE calculated using a Bordwell cycle as discussed in ref. 29b: (a) pKa in DMSO: Bordwell FG, Cheng J. J. Am. Chem. Soc 1991;113:1736–1743.1743 pKa converted from DMSO to CH_3CN following: (b)Kutt A, Kaljurand I, Sooväli L, Vlasov VM, Yagupolskii LM, Koppel IA. J. Org. Chem 2006;71:2829–2838.2838 [PubMed: 16555839] $E_{½}$ vs. Cp_2Fe^+/Cp_2Fe in CH_3CN from: (c) Niyazymbetov ME, Evans DH. J. Chem. Soc. Perkin Trans.2 1993;7:1333–1338.1338 (d) Solution BDFEs are also discussed in reference 66.
55. Wu A, Maslan J, Swartz RD, Kaminsky W, Mayer JM. Inorg. Chem 2007;46:11190–11201. [PubMed: 18052056]
56. (a) In similar oxidations by metal coordination complexes, we have found that the production of anthrone or xanthone depends on the rate of trapping of the benzylic radical.27,28,56b,c, This trapping may be slow due to the low oxidizing power of the vanadium(VI) hydroxide species (discouraging radical rebound), and due to the high intrinsic barrier to oxidation in this system. With slow trapping of R•, the reactions proceed to form anthracene or bixanthenyl. (b)Larsen AS, Wang K, Lockwood MA, Rice GL, Won TJ, Lovell S, Sadilek M, Turecek F, Mayer JM. J. Am. Chem. Soc 2002;124:10112–10123.10123 [PubMed: 12188675] (c)Wang K, Mayer JM. J. Am. Chem. Soc 1997;119:1470–1471.1471
57. BDEs were converted to BDFEs following ref 29b
58. (a) Becke AD. J. Chem. Phys 1993;98:5648. (b) Lee C, Yang W, Parr RG. Phys. Rev. B 1998;37:785.
59. Hariharan PC, Pople JA. Theor. Chim. Acta 1973;28:213.
60. (a) Miertus S, Scrocco E, Tomasi J. Chem. Phys 1981;55:117. (b) Miertus S, Tomasi J. Chem. Phys 1982;65:239.
61. Frisch MJ, et al. Gaussian 03, Revision C.02. 2004Wallingford CTGaussian Inc. The full list of authors is given in the Supporting Information.
62. Mayer JM. Inorg. Chem 1988;27:3899–3903.
63. Two other transition structures for **1c** + **2c**, with C_i and C_s symmetry, were also located. They were computed to be, respectively, 6.9 and 6.7 kcal/mol higher in enthalpy than the C_2transition structure. Thus, the transition structure that involves two molecules of the same chirality is computed to be considerably lower in energy than either of the two transition structures that involve molecules of opposite chirality.
64. (a) For these calculations, the relativistic, compact effective potential and basis set of Stevens, Basch, Krauss, and Jasien was used for ruthenium64b and 6–31G(d) was used for all of the other atoms. Stevens WJ, Krauss M, Basch H, Jasien PG. Can. J. Chem 1992;70:612.
65. Calculations on the isolated molecules were performed on the doublet states of the ruthenium hydroxy species and on the triplet states of the ruthenium oxo species, because the quartet state was found to be lowest for both the hydrogen-bonded complexes and for the transition structures.
66. (a) BDFEs are used, rather than the more common bond dissociation enthalpies (BDEs) because recent studies of metal-mediated hydrogen transfer reactions have shown that entropies of reaction ($\Delta S°$) can be large in magnitude and should not be ignored.29,66b, Mader EA, Manner VW, Markle TF, Wu A, Franz JA, Mayer JM. submitted.
67. Friedrich LE. J. Org. Chem 1983;48:3851–3852.
68. Borges dos Santos RM, Martinho Simoes JA. J. Phys. Chem. Ref. Data 1998;27:707–739.
69. These reactions are different from H-transfer reactions of metal hydrides; see, for instance: (a)Choi J, Pulling ME, Smith DM, Norton JR. J. Am. Chem. Soc 2008;130:4250–4252.4252 [PubMed: 18335937] (b)Choi J, Tang L, Norton JR. J. Am. Chem. Soc 2007;129:234–240.240 and references therein. [PubMed: 17199304] (c)Edidin RT, Sullivan JM, Norton JR. J. Am. Chem. Soc 1987;109:3945–3953.3953 (d)Bullock RM. Transition Metal Hydrides 1992New YorkVCH:263–304.304 (e)Protasiewicz JD, Theopold KH. J. Am. Chem. Soc 1993;115:5559–5569.5569 (f)Song J-S, Bullock RM, Creutz C. J. Am. Chem. Soc 1991;113:9862–9864.9864 Creutz C, Song J-S, Bullock RM. Pure Appl. Chem 1995;67:47–54.54 (g)Bakac A. Inorg. Chem 1998;37:3548–3552.3552 [PubMed: 11670442] (h)Fu X, Wayland BB. J. Am. Chem. Soc 2005;127:16460–16467.16467 [PubMed: 16305232]
70. Roth JP, Lovell S, Mayer JM. J. Am. Chem. Soc 2000;122:5486–5498.

NIH-PA Author Manuscript NIH-PA Author Manuscript NIH-PA Author Manuscript

71. Litwinienko G, Ingold KU. Acc. Chem. Res 2007;40:222–230. [PubMed: 17370994]
72. (a)Boas LV, Pessoa JC. Wilkinson G, Gillard RD, McCleverty JA. Comprehensive Coordination Chemistry 1987;3New YorkPergamon:453–583.583 (b)Crans DC, Smee JJ. McCleverty JA, Meyer TJ. Comprehensive Coordination Chemistry II From Biology to Nanotechnology 2004;4BostonElsevier Pergamon:175–239.239 (c) *E.g.*, $V^{V}(O)(OH)^{2+}$ (aq) is estimated to have a pK_a of −1.5 but has not been observed and hydrolysis of $V^{IV}O^{2+}$ does not give dioxo species.72d,e (d)Macartney DH. Inorg. Chem 1986;25:2222–2225.2225 (e)Richens DT. The Chemistry of Aqua Ions 1997New YorkJohn Wiley and Sons:234–243.243 (f) See also references 20–24.
73. The $E_{½}$ for the one electron oxidation of xanthene is 1.15 in DMSO: Chen J, Lu Y, Zhu X, Mu L. J. Org. Chem 1998;63:6108–6114.6114 [PubMed: 11672236]
74. The $E_{½}$ for $TEMPOH^{0/+\bullet}$ in MeCN is 0.71 ± 0.02 V (converted from $Ag/AgNO_3$ to $FeCp_2^{0/+}$ by subtracting 0.088 V): Semmelhack MF, Chou CS, Cortes DA. J. Am. Chem. Soc 1983;105:4492–4494.4494
75. Irreversible oxidation of hydroquinone in MeCN occurs at 0.73 V (converted from SCE to $FeCp_2^{0/+}$ by subtracting 0.40 V): Parker VD. J. Chem. Soc., Chem. Comm 1969:716–717.717
76. Bordwell FG, Liu WZ. J. Am. Chem. Soc 1996;118:10819–10823.
77. (a) The pK_a of xanthene and dihydroanthracene are reported as 30.1 in: Bordwell FG, Cheng J, Ji G, Satish AV, Zhang X. J. Am. Chem. Soc 1991;113:9790–9795.9795 (b) The above p*K*a's in DMSO can be converted to a pK_a in CH_3CN following: Wayner DDM, Parker VD. Acc. Chem. Res 1993;26:287–294.294
78. Wagner PJ, Zhang Y, Puchalski AE. J. Phys. Chem 1993;97:13368–13374.
79. (a) Iordanova N, Decornez H, Hammes-Schiffer S. J. Am. Chem. Soc 2001;123:3723–3733. [PubMed: 11457104] (b) Hammes-Schiffer S. Acc. Chem. Res 2001;34:273–281. [PubMed: 11308301] (c) Hatcher E, Soudackov A, Hammes-Schiffer S. J. Phys. Chem. B 2005;109:18565–18574. [PubMed: 16853391]
80. Benson, SW. Thermochemical Kinetics. Vol. 2nd ed.. New York: Wiley; 1976. (b) Foti M, Ingold KU, Lusztyk J. J. Am. Chem. Soc 1994;116:9440–9447.
81. See, for instance, discussions in references 46b, 79, 95, and 96.
82. Marcus RA, Sutin N. Biochim. Biophys. Acta 1985;811:265–322.
83. f_{xy}82 is usually close to 1.
84. Mader EA, Mayer JM. to be submitted.
85. Eberson, L. Electron Transfer Reactions in Organic Chemistry. Berlin Heidelberg: Springer-Verlag; 1987. Chapter 3.
86. Wu A, Datta A, Hrovat DA, Borden WT, Mayer JM. manuscript in preparation
87. Bryant, JR. Ph. D. Thesis. Seattle, WA: University of Washington; 2002 Dec.
88. Warren JJ, Mayer JM. manuscript in preparation
89. (a) We also performed calculations with the MPW1K functional.89b The energies for all of the steps in Figure 8 computed with MPW1K/6–31+G(d,p) were similar to those computed with B3LYP/6–31G(d), except for the hydrogen transfer step (**c→d**). The MPW1K calculations gave values about 10 kcal mol^{-1} higher for the vanadium complex and 7–8 kcal mol^{-1} higher for the ruthenium complexes. The barrier heights computed with MPW1K were higher than B3LYP values by 12.8 kcal mol^{-1} for VO_2/V(O)OH and by 11.6 and 10.4 kcal mol^{-1} for RuO(pyrr)/Ru(OH)(pyrr) and RuO(F)/Ru(OH)(F) respectively. Probably through a fortuitous cancellation of errors, the B3LYP barrier heights are in much better agreement with experiment than are the MPW1K barrier heights. Lynch BJ, Fast PL, Harris M, Truhlar DG. J. Phys. Chem. A 2000;104:4811.
90. The V-OH bond of 1c is ~0.2 Å shorter than a typical Ru^{III}-OH bond [a structure of $Ru^{III}OH(bpy)_2(py)^{2+}$ has not been reported]: (a)Man ML, Zhu J, Ng SM, Zhou Z, Yin C, Lin Z, Lau CP. Organometallics 2004;23:6214–6220.6220 (b)Jitsukawa K, Oka Y, Yamaguchi S, Masuda H. Inorg. Chem 2004;43:8119–8129.8129 [PubMed: 15578852] (c)Takahashi Y, Hikichi S, Moro-oka Y, Akita M. Polyhedron 2004;23:225–234.234 (d)Nagao H, Aoyagi K, Yukawa Y, Howell FS, Mukaida M, Kakihana H. Bull. Chem. Soc. Jpn 1987;60:3247–3245.3245 (e)Gibson DH, Pariya C, Mashuta MS. Organometallics 2004;23:2510–2513.2513 (f)Gemel C, Mereiter K, Schmid R, Kirchner K. Organometallics 1997;16:5601–5603.5603 (g)Schneider R, Weybermüller T, Wieghardt K. Inorg.

NIH-PA Author Manuscript

NIH-PA Author Manuscript

NIH-PA Author Manuscript

Chem 1993;32:4925–4934.4934 (h)Anderson C, Beauchamp AL. Inorg. Chem 1995;34:6065–6073.6073

91. V=O bonds62 are ca. 0.16 Å shorter than corresponding Ru^{IV}=O bonds [a structure of $Ru^{IV}O(bpy)_2(py)^{2+}$ has not been reported]: (a)Che C, Lai T, Wong K. Inorg. Chem 1987;26:2289–2299.2299 and refs. therein. (b)Che C, Tang W, Lee W, Wong W, Lai T. J. Chem. Soc. Dalton. Trans 1989:2011–2016.2016 (c)Wong K, Che C, Yip W, Wang R, Mak TCW. J. Chem. Soc. Dalton. Trans 1992:1417–1421.1421
92. (a) Moyer BA, Meyer TJ. J. Am. Chem. Soc 1978;100:3601–3603. (b) Aoyagi K, Yukawa Y, Shimuzu K, Mukaida M, Takeuchi T, Kakihana H. Bull. Chem. Soc. Jpn. J. Am. Chem. Soc 1986;59:1493–1499. (c) Marmion ME, Takeuchi KJ. J. Am. Chem. Soc 1986;108:510–511.
93. In a three-electron π bond, the electron that occupies the antibonding orbital more than cancels the bonding contributed by one of the electrons in the bonding orbital. See, for example, Jorgensen WL, Borden WT. J. Am. Chem. Soc 1973;95:6649.
94. Binstead RA, McGuire ME, Dovletoglou A, Seok WK, Roecker LE, Meyer TJ. J. Am. Chem. Soc 1992;114:173–186.186 (a) See also reference 1.
95. (a) Mayer JM, Hrovat DA, Thomas JL, Borden WT. J. Am. Chem. Soc 2002;124:11142–11147. [PubMed: 12224962] (b) Lingwood M, Hammond JR, Hrovat DA, Mayer JM, Borden WT. J. Chem. Theory and Comput 2006;2:740–745. [PubMed: 18725967]
96. Tishchenko O, Truhlar DG, Ceulemans A, Nguyen MT. J. Am. Chem. Soc 2008;130:7000–7010. [PubMed: 18465862]
97. Binstead RA, Meyer TJ. J. Am. Chem. Soc 1987;109:3287–3297.3297 The emphasis is in the original. This definition of HAT precedes Meyer's different definition (quoted above) in references 1 and 94.
98. http://www.glasscontoursolventsystems.com/index.php/about
99. Modarelli DA, Rossitto FC, Lahti PM. Tetrahedron Lett 1989;30:4473–4476.

NIH-PA Author Manuscript
NIH-PA Author Manuscript
NIH-PA Author Manuscript

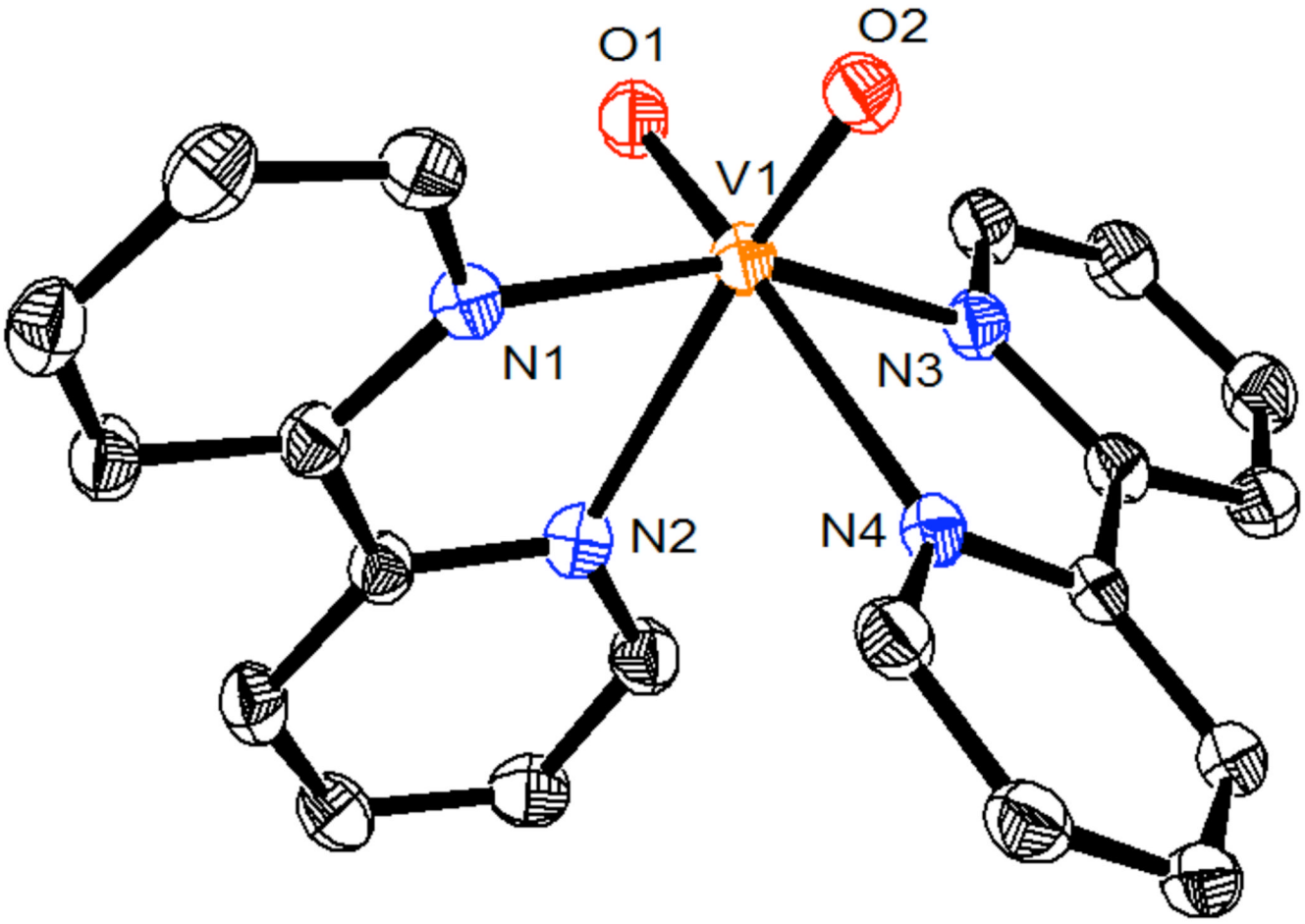

Figure 1.
ORTEP of the cation in $[V^{V}O_2(bpy)_2]BF_4$ (**2c**), with hydrogen atoms omitted for clarity.

NIH-PA Author Manuscript
NIH-PA Author Manuscript
NIH-PA Author Manuscript

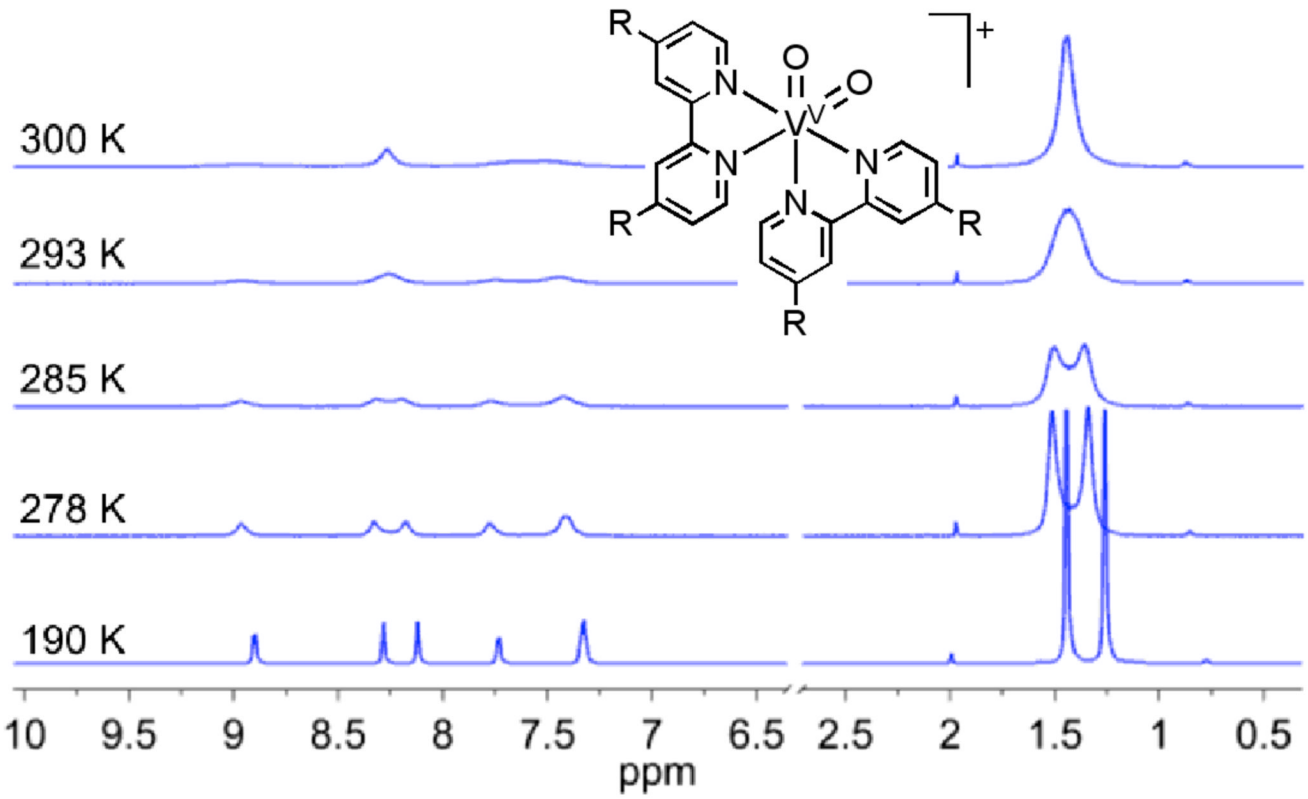

Figure 2.
Variable temperature ^{1}H NMR spectra of **2a** in CD_2Cl_2, R = ^{t}Bu.

NIH-PA Author Manuscript

NIH-PA Author Manuscript

NIH-PA Author Manuscript

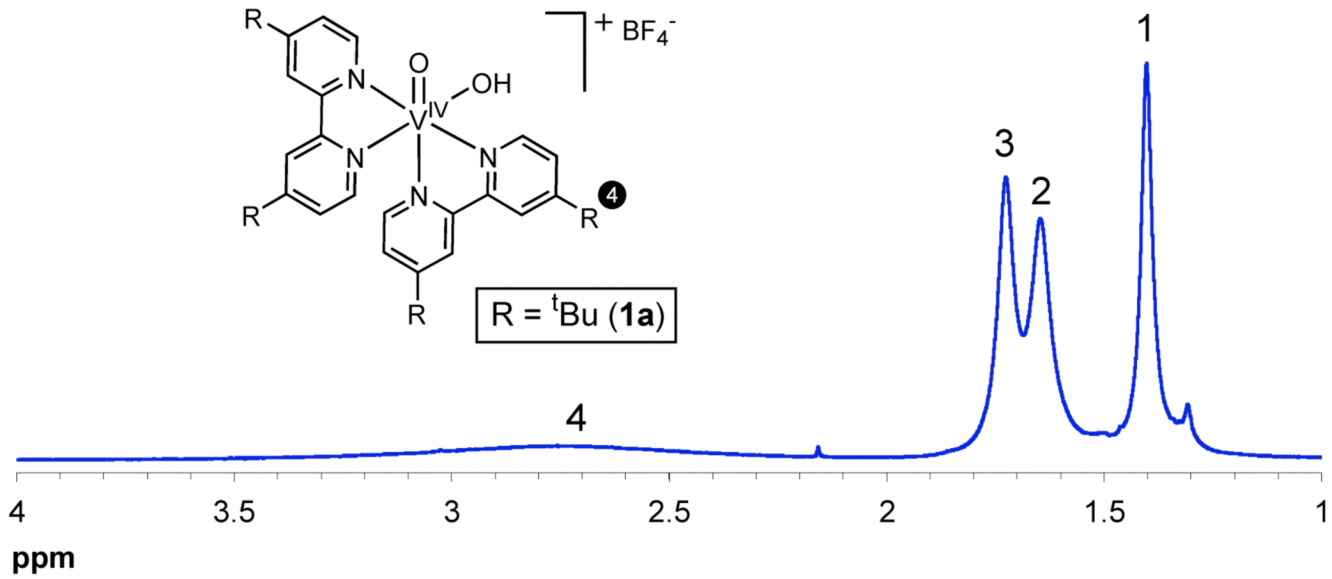

Figure 3.
^{1}H NMR of **1a** in CD_2Cl_2 with the ^{t}Bu peaks noted 1–4.

NIH-PA Author Manuscript

NIH-PA Author Manuscript

NIH-PA Author Manuscript

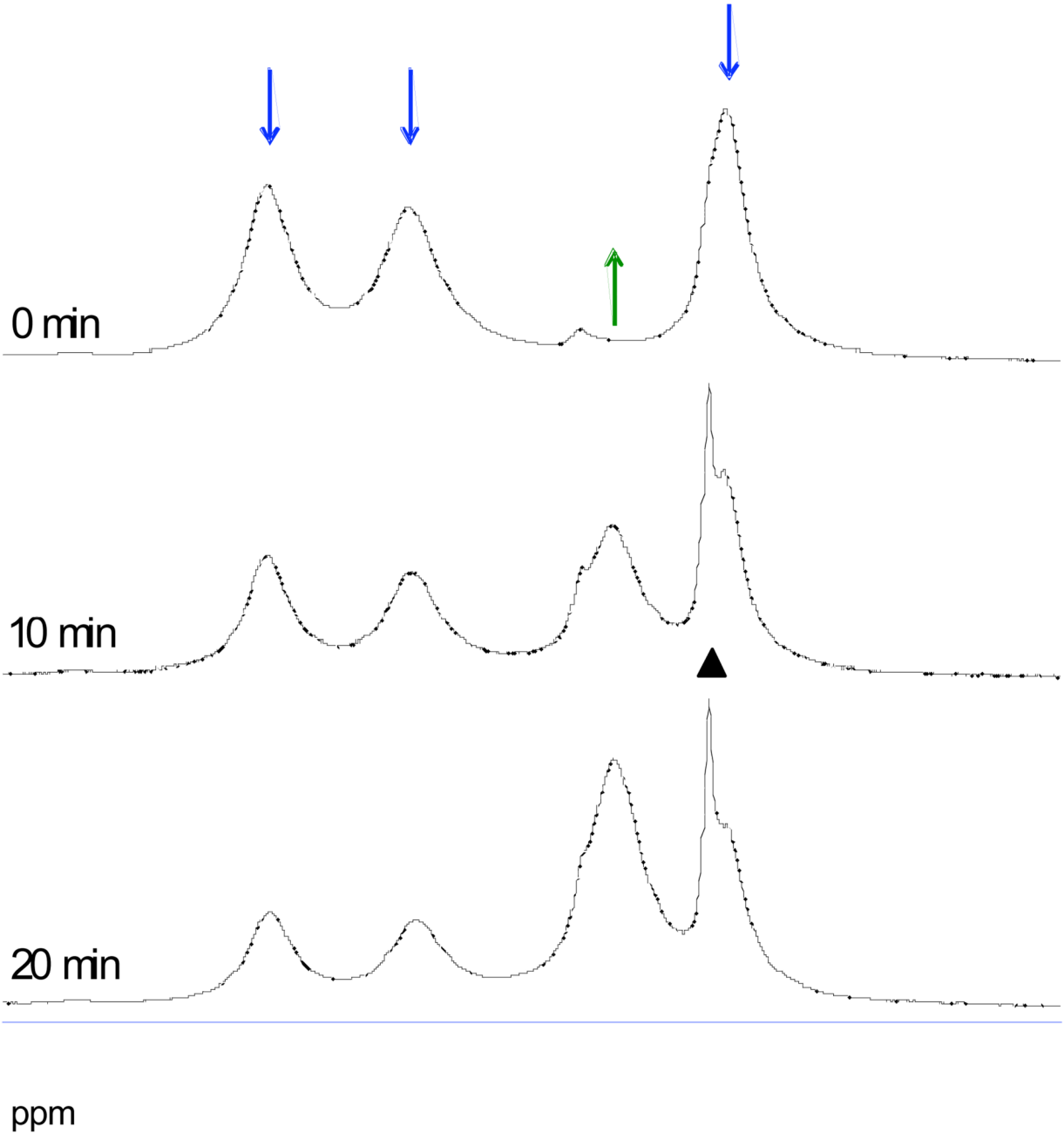

Figure 4.
^{t}Bu region of ^{1}H NMR spectra of the of pseudo self-exchange reaction between **1a** and **2b** at 320 K in CD_3CN; ▲ denotes free $^{t}Bu_2bpy$.

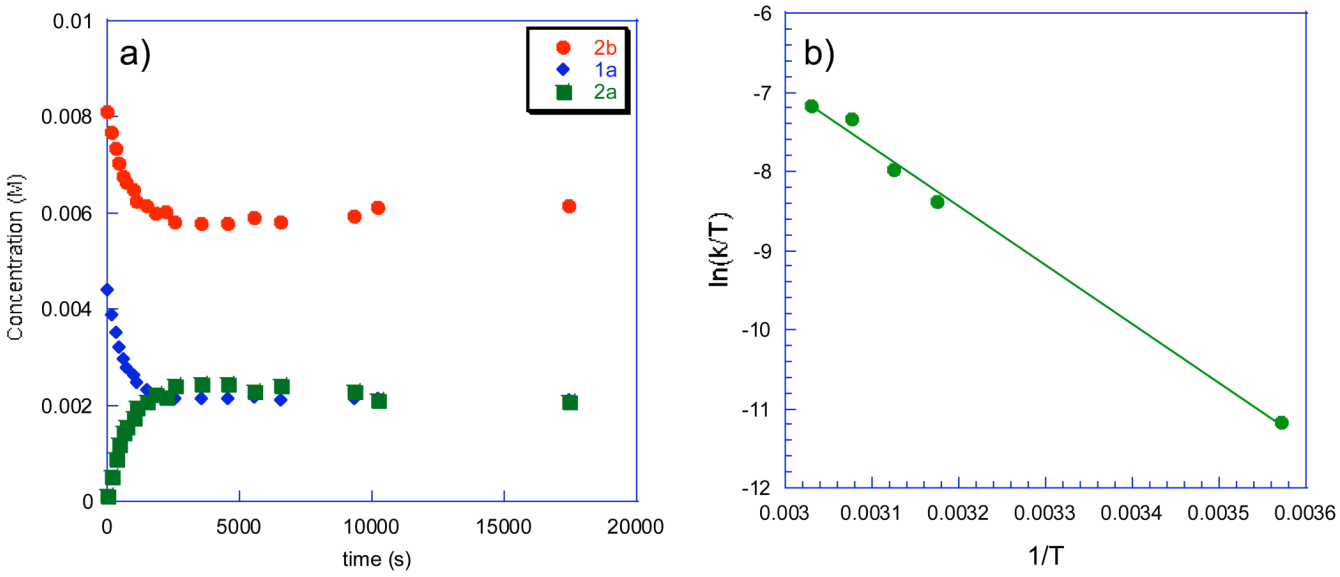

Figure 5.

(a) Plot of the concentrations vs. time for the pseudo-self-exchange reaction of **1a** and **2b** in CD_3CN at 320 K. (b) Eyring plot of pseudo self-exchange rate constants.

NIH-PA Author Manuscript NIH-PA Author Manuscript NIH-PA Author Manuscript

NIH-PA Author Manuscript
NIH-PA Author Manuscript
NIH-PA Author Manuscript

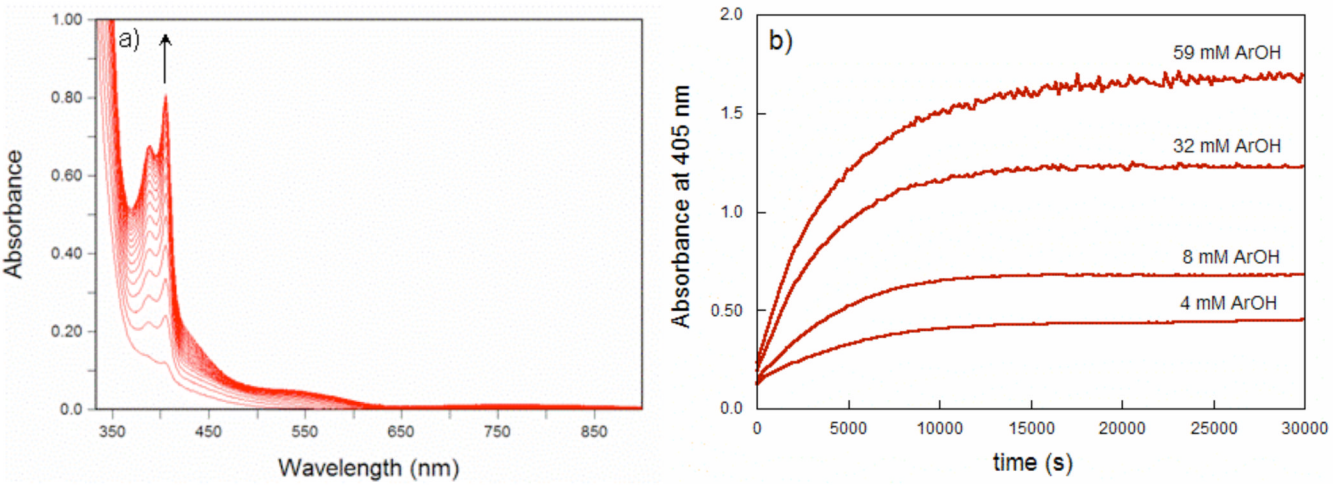

Figure 6.

(a) Optical spectra and (b) absorbance vs. time plots for the reaction of **2a** (1.6 mM) with $^{t}Bu_2(MeO)C_6H_2OH$ in CH_3CN at 298 K.

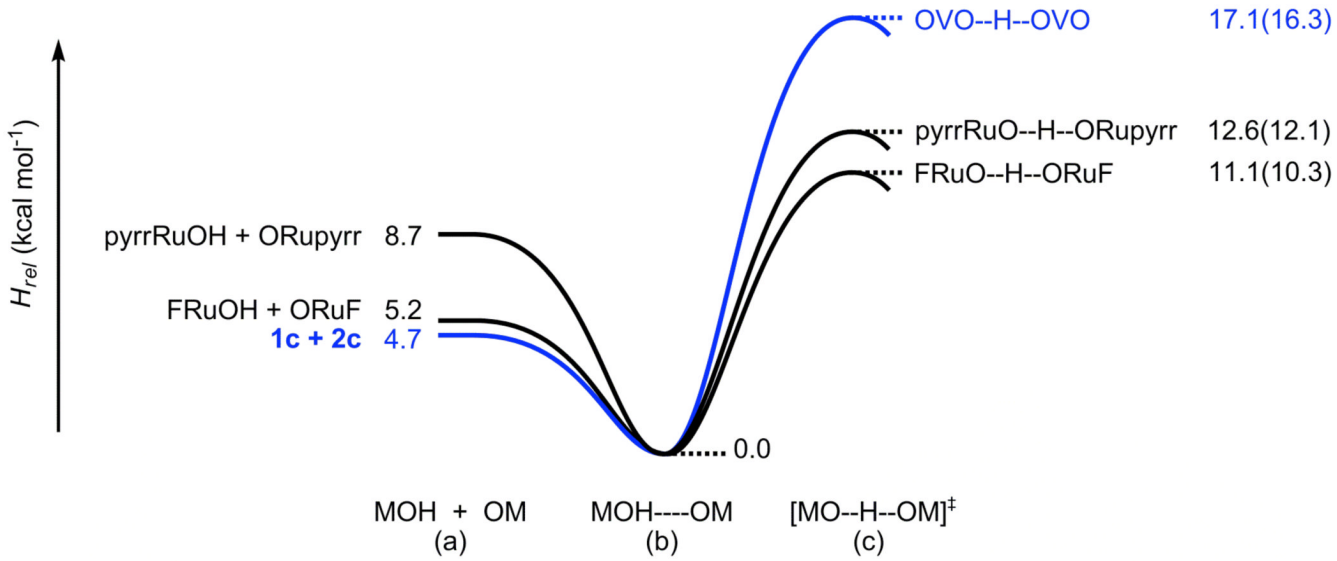

Figure 7.
B3LYP/6–31G* PCM enthalpies (kcal mol^{-1}), relative to the hydrogen-bonded complexes (b), of the reactants (a) and transition structures (c) in three degenerate hydrogen exchange reactions in acetonitrile solution. For the transition structures, the gas-phase enthalpies are given in parentheses.

NIH-PA Author Manuscript NIH-PA Author Manuscript NIH-PA Author Manuscript

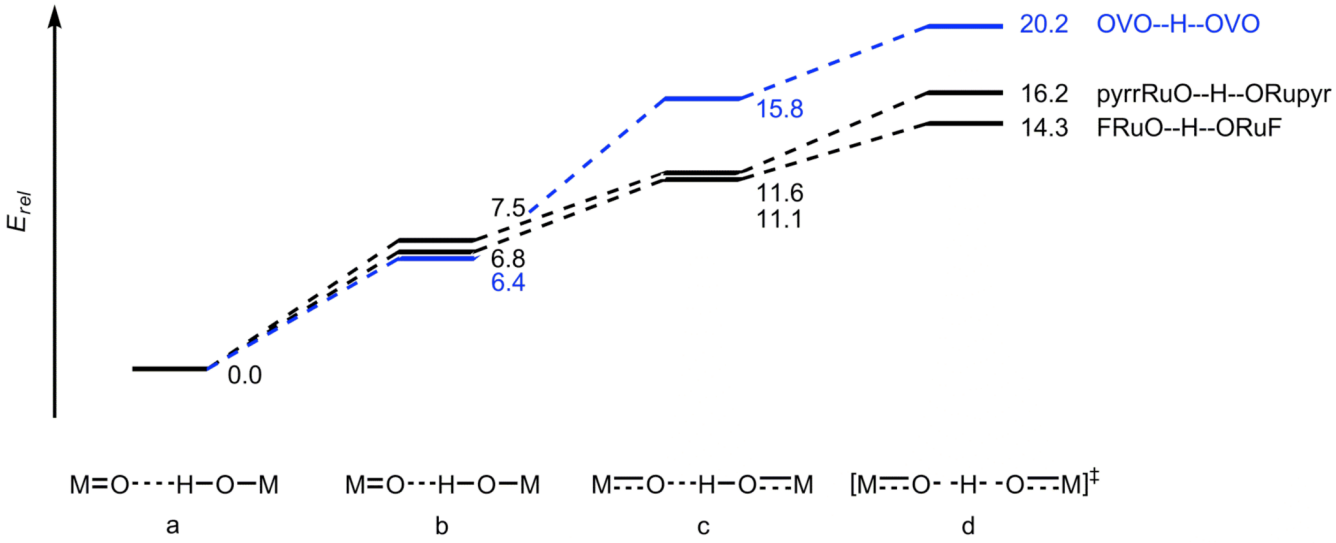

Figure 8.

Relative gas-phase energies (ΔE in kcal mol^{-1}) of: (**a**) the optimized hydrogen bonded precursor complexes (E set equal to 0); (**b**) the O···O distances shortened to those in the transition structures, but all other geometrical parameters optimized; (**c**) all of the atoms moved to their positions in the transition structures, except for the transferring proton, whose position was optimized; and (**d**) the optimized transition structures.

NIH-PA Author Manuscript NIH-PA Author Manuscript NIH-PA Author Manuscript

NIH-PA Author Manuscript

NIH-PA Author Manuscript

NIH-PA Author Manuscript

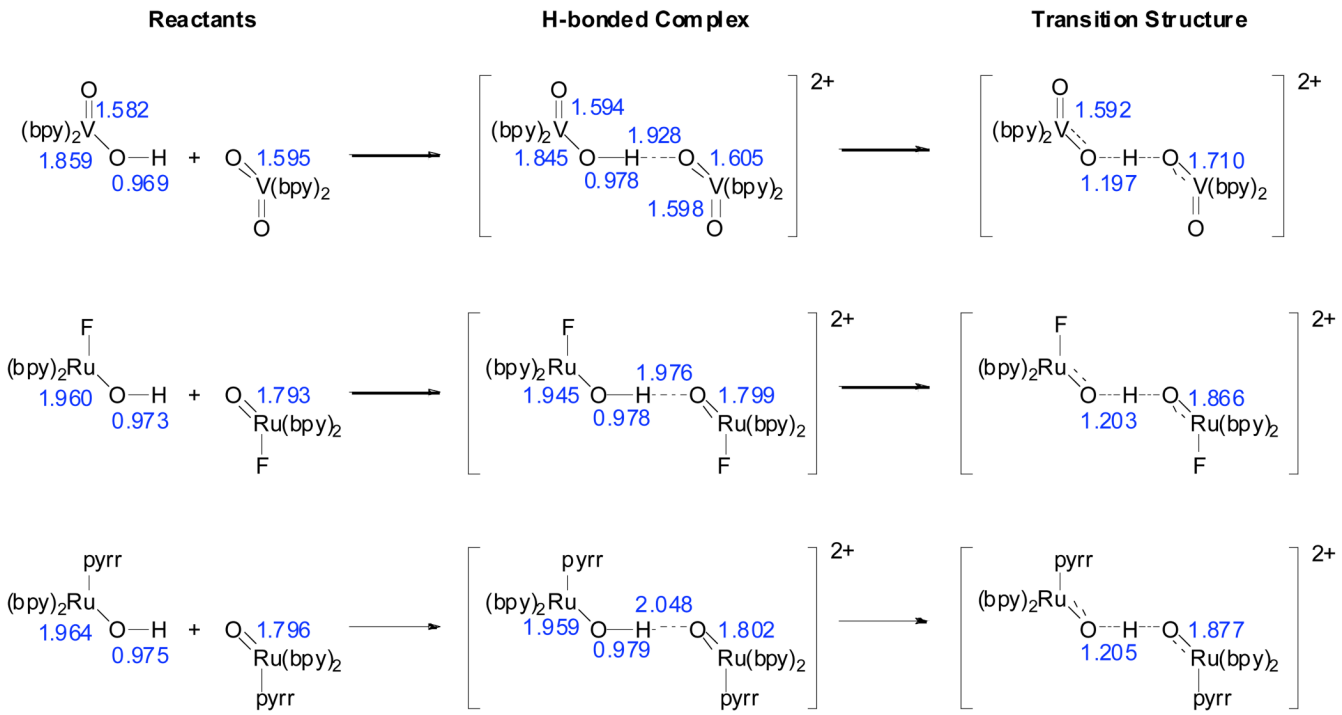

Figure 9.
M=O, M-OH, and O-H bond lengths (Å) in the reactants, hydrogen-bonded complexes, and transition structures for three hydrogen atom self-exchange reactions.

NIH-PA Author Manuscript

NIH-PA Author Manuscript

NIH-PA Author Manuscript

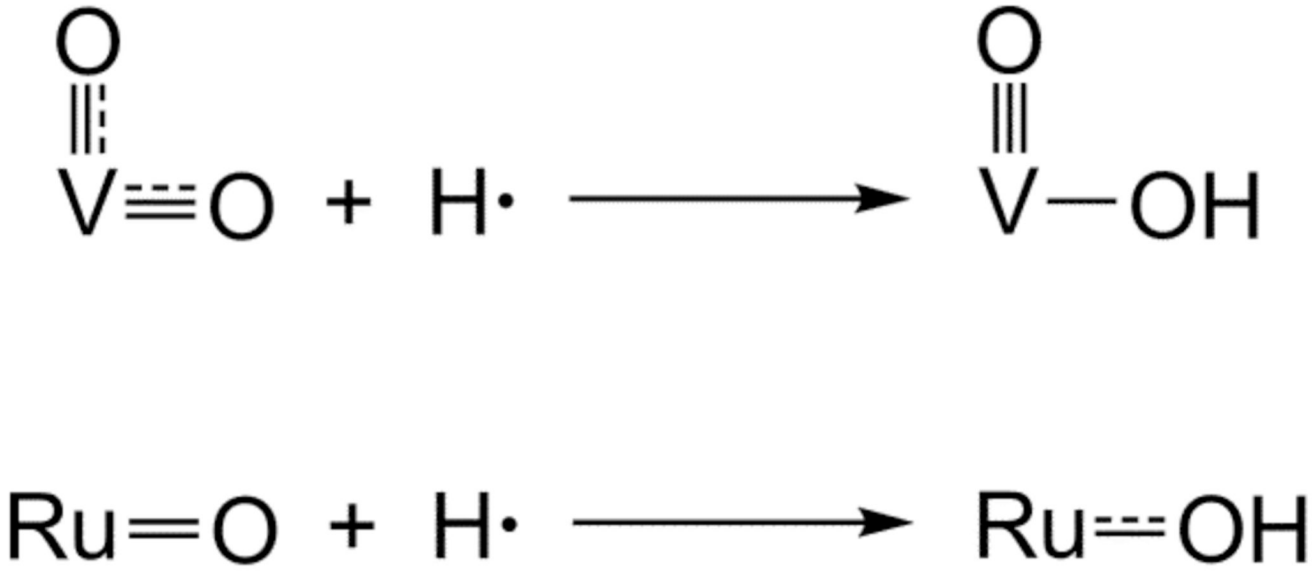

Figure 10.
Summary of changes in π bonding upon addition of a hydrogen atom to **2a–c** or to [Ru^{IV}(O)(L)$(bpy)_2$].

NIH-PA Author Manuscript
NIH-PA Author Manuscript
NIH-PA Author Manuscript

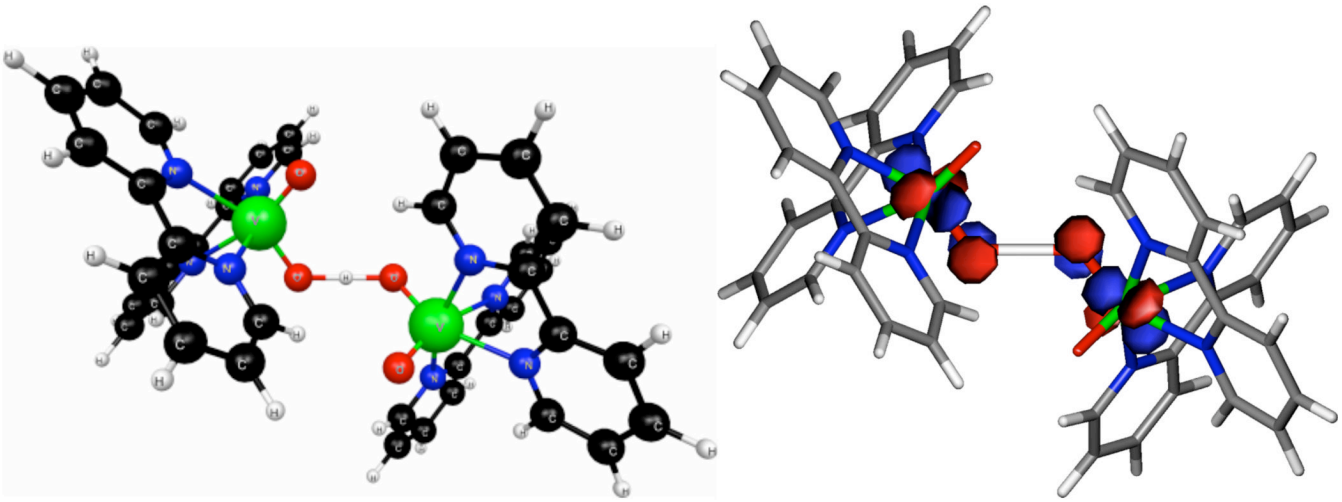

Figure 11.
Computed structure (left) and SOMO (right) of the **1c + 2c** transition structure. The V-O-O-V dihedral angle is 118.4°.

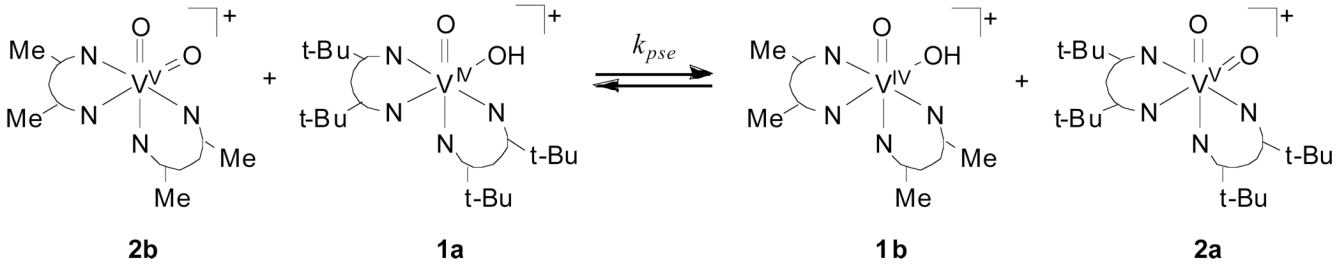

2b **1a** **1b** **2a**

Scheme 1.
Hydrogen atom pseudo self-exchange reaction

NIH-PA Author Manuscript
NIH-PA Author Manuscript
NIH-PA Author Manuscript

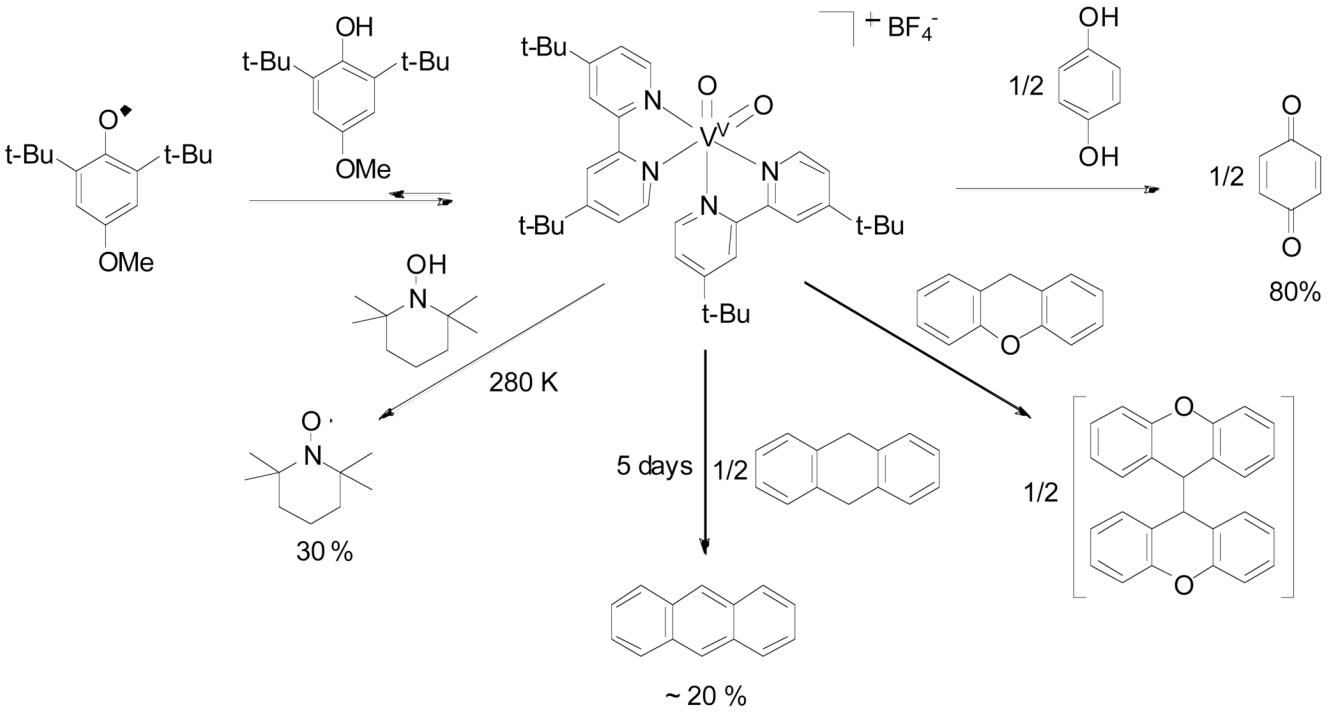

Scheme 2.
Summary of the reactivity of **2a** with hydrogen atom donors.

NIH-PA Author Manuscript NIH-PA Author Manuscript NIH-PA Author Manuscript

NIH-PA Author Manuscript NIH-PA Author Manuscript NIH-PA Author Manuscript

Table 1

Calculated and solid-state bond lengths (Å) and angles (°) for $[V^{IV}O(OH)(bpy)_2]^+$ (**1c**), $[V^{V}O_2(bpy)_2]^+$ (**2c**), and the transition structure for self-exchange.

	$[V^{IV}O(OH)(bpy)_2]^+$ (1c)		$[V^{V}O_2(bpy)_2]^+$ (2c)		VO···H···OV Transition Structure[a]
	Calculated[a]	Solid-State[b]	Calculated[a]	Solid-State[c]	
V–O(1)	1.582	1.687(2)	1.595	1.6234(14)	1.592
V–O(2)	1.859	1.761(2)		1.6301(14)	1.710
V–N(1)	2.152	2.115(3)	2.160	2.1102(17)	2.144
V–N(3)	2.172	2.111(3)		2.1179(17)	2.348
V–N(2)	2.228	2.175(3)	2.350	2.2778(18)	2.175
V–N(4)	2.378	2.247(3)		2.2412(16)	2.113
O–H	0.969	-	-	-	1.197
O–V–O	109.5	106.8(12)	107.4	106.41(7)	107.42

[a] Gas phase calculation.

[b] Reference 18a; BF_4 salt.

[c] This work; BF_4 salt.

J Am Chem Soc. Author manuscript; available in PMC 2010 April 8.

NIH-PA Author Manuscript

NIH-PA Author Manuscript

NIH-PA Author Manuscript

Table 2

Driving force and second-order rate constants for transfer of a hydrogen atom from organic substrates to $[V^{V}O_2(^{t}Bu_2bpy)_2]^{+}$ (**2a**).

Reaction	$\Delta G°$ (kcal mol^{-1})[a]	k(M^{-1} s^{-1})	T(K)
2a + TEMPOH	−4.1 ± 1.0	~1 × 10^{-1}	275
2a + xanthene	0.3 ± 1.0	(7.6 ± 2.4) × 10^{-5}	298
2a + ^{t}Bu$_2$(MeO)ArOH	3.3 ± 0.5	(1.4 ± 0.5) × 10^{-2}	298
2a + DHA	2.8 ± 1.0	~ 2 × 10^{-6}	298
2a + hydroquinone	7.0 ± 1.0	(4.0 ± 0.5) × 10^{-2}	298

[a] $\Delta G°$ for transfer of the first H from the substrate to **2a**, calculated from BDFE values,[28,29,51,53–57,68] except for the reaction with ^{t}Bu$_2$(MeO)ArOH that was measured directly.

NIH-PA Author Manuscript

NIH-PA Author Manuscript

NIH-PA Author Manuscript

Table 3

Measured and estimated NH and OH hydrogen atom self-exchange rate constants, k_{se} for XH + X ⇌ X + HX, statistically corrected.[a]

XH	Measured k_{se}	Estimated k_{se}[b]	Reference
$Fe^{II}(H_2bim)_3^{2+}$[c]	$(9.7 \pm 1.0) \times 10^2$		70
$Fe^{II}(H_2bip)_3^{2+}$[c]	$(2.2 \pm 0.3) \times 10^3$		30
$TpOs^{III}(NH_2Ph)Cl_2$[c]	$(1.5 \pm 1) \times 10^{-3}$		31
$Ru^{II}(acac)_2(py\text{-}imH)$	$(3.2 \pm 0.3) \times 10^5$		46
$Ru^{III}(bpy)_2(py)(OH)^{2+}$	$(7.6 \pm 0.4) \times 10^4$		28a
$[Mn^{VI}(OH)O_3^-]$		$\sim 2 \times 10^6$[d]	
$[(phen)_2Mn^{III}(\mu\text{-}OH)(\mu\text{-}O)Mn^{III}(phen)_2]^{3+}$	-	$\sim 4 \times 10^3$[e]	
$[(phen)_2Mn^{III}(\mu\text{-}OH)_2Mn^{II}(phen)_2]^{3+}$	-	$\sim 3 \times 10^5$[e]	
$[Cr^V(OH)OCl_2]$	-	$\sim 2 \times 10^3$[f]	
$\bullet CR_2(OH)$ [g]	$(3.7\text{–}8.6) \times 10^3$		78
$V^{IV}O(OH)(R_2bpy)^+$	$(6.5 \pm 0.1) \times 10^{-3}$		This work

[a] k_{se}(M^{-1} s^{-1}) at 298 K, in MeCN unless otherwise indicated; all rates statistically corrected by dividing the observed self-exchange rate by the number of X-H donor sites and/or H• acceptor sites as necessary.

[b] Estimated from the Marcus cross relation using known $\Delta G°$, observed k_{HAT} and k_{se} of the organic reagent.[39]

[c] H_2bim = 2,2′-biimidazoline; H_2bip = 2,2′-bi(tetrahydropy-rimidine); Tp = hydrotris(pyrazolyl)borate.

[d] Estimated from the rate of DHA oxidation reported in ref [27e].

[e] Estimated from the rate of DHA oxidation reported in refs. [56b,c]

[f] Estimated from the rate of oxidation of neat toluene reported in [27c]

[g] Rates measured in benzene.

NIH-PA Author Manuscript NIH-PA Author Manuscript NIH-PA Author Manuscript

Table 4

Calculated and observed hydrogen atom transfer rate constants (statistically corrected) and equilibrium constants for reactions of $VO_2(^tBu_2bpy)_2^{2+}$ (**2a**) with organic substrates.

Reaction	T (K)	K_{eq} [a]	K_{yy} (M^{-1} s^{-1})	K_{calc} (M^{-1} s^{-1}) [b]	K_{xy} (M^{-1} s^{-1})	K_{xy}/K_{calc}
2a + TEMPOH	275	1.0×10^{3} [c]	2.3 ± 1.0 [d]	2	~1×10^{-1} [d]	20
2a + xanthene	298	6.0×10^{-1}	~5×10^{-11} [e]	5×10^{-7}	$(3.8 \pm 1.2) \times 10^{-5}$ [f]	80
2a + $^tBu_2$(MeO)ArOH	298	3.8×10^{-3}	2.0×10^{1} [g]	3×10^{-2}	$(1.4 \pm 0.5) \times 10^{-3}$	0.05
2a + DHA [f]	298	8.8×10^{-3}	~5×10^{-11} [e]	6×10^{-8}	~2×10^{-7} [f]	3
2a + hydroquinone [f]	298	7.4×10^{-6}	3×10^{4} [h]	4×10^{-2}	$(1 \pm 0.5) \times 10^{-2}$ [f]	0.2

[a] K_{eq} calculated from $\Delta G°$ values in Table 2, with estimated errors ± a factor of ten, except for the reaction with $^tBu_2$(MeO)ArOH that was measured directly.

[b] k_{calc} from eq 7, using k_{XX}(**1a+2a**) = 1.3×10^{-3} M^{-1} s^{-1} at 275 K and 6.5×10^{-3} M^{-1} s^{-1} at 298 K (Table 3). The estimated errors on k_{calc} are at least a factor of ten (see text).

[c] Assumed equal to K_{eq} at 298 K.

[d] k_{yy}(TEMPOH) at 275 K from refs 29a, 86.

[e] Uses k_{yy}(DHA) extracted from reaction of DHA with $Fe(Hbim)(H_2bim)_2^{3+}$.87

[f] Statistical corrections: for xanthene and hydroquinone, k_{xy} = ½k_{obs} due to two reactive substrate H atoms; for DHA, k_{xy} = ⅛k_{obs} due to four reactive H atoms and the stoichiometry of two **2a** per DHA oxidized.

[g] Pseudo self-exchange rate constant for reaction of 2,4,6-$^tBu_3$PhO• + 2,6-^{t}Bu-4-MePhOH in MeCN.88

[h] Ref. 30.

J Am Chem Soc. Author manuscript; available in PMC 2010 April 8.